ACS BIO & MED CHEM Au
AN OPEN ACCESS JOURNAL OF THE AMERICAN CHEMICAL SOCIETY

Editors' Choice
Open Access

pubs.acs.org/biomedchemau
Article

Glycosylated *N*-Acyl Phosphoethanolamines as Bacterial Food-Dependent Signaling Molecules in *Caenorhabditis* Nematodes

Siva Bandi,[‖] Marie-Désirée Schlemper-Scheidt,[‖] Rocío Rivera Sánchez, Sylvain Sutour, Gaétan Glauser, Yojiro Ishida, and Stephan H. von Reuß*

Cite This: *ACS Bio Med Chem Au* 2025, 5, 602–619
Read Online

ACCESS | Metrics & More | Article Recommendations | Supporting Information

ABSTRACT: *N*-acyl ethanolamines represent conserved lipophilic signaling molecules that function as endogenous ligands at G-protein-coupled receptors, ion channels, and nuclear receptors. Using a combination of comparative ultrahigh-performance liquid chromatography electrospray ionization high-resolution tandem mass spectrometry (UHPLC-ESI-HR-MS^E) analysis and micro-reactions, a diversity of glycosylated *N*-acyl phosphoethanolamines were characterized in *Caenorhabditis* nematodes. Representative examples were enriched by RP-C18 chromatography and identified by NMR spectroscopy. Comparative metabolomics and isotope incorporation experiments revealed that the biosynthesis of the homologous *N*-acyl building blocks (approximately 50 compounds) depends on the bacterial food source, chain elongation and desaturation of food-derived fatty acids, or their de novo biosynthesis by the nematode, whereas the biosynthesis of medium-chain *N*-acyl units depends on the peroxisomal *β*-oxidation cycle via the 3-ketoacyl-*S*-CoA thiolase *daf-22*. Glycosylation of these lipophilic *N*-acyl ethanolamines results in amphiphilic modular metabolites (approximately 100 identified compounds) that are released into the environment and exhibit potential signaling functions. Exclusively male-produced *β*-sophorosyl *N*-acyl-phosphoethanolamines like SNAP-13:1cyclo retain females of *Caenorhabditis wallacei* and *Caenorhabditis brenneri*, and its biosynthesis requires bacterial cyclo fatty acids 17:1cyclo and 19:1cyclo, thereby translating growth phase-dependent bacterial lipogeneses into a behavioral signal. Amphiphilic 2-(*β*-glucosyl)-glyceryl *N*-eicosapentaenoyl phosphoethanolamine (GGp-NAE-20:5), a dominating component of the *Caenorhabditis elegans* metabolome, represents a water-soluble derivative of *N*-eicosapentaenoyl ethanolamine (NAE 20:5), potentially enabling intra- and interspecies endocannabinoid signaling.

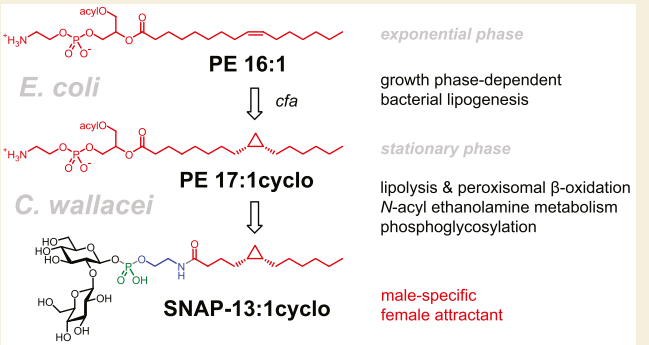

KEYWORDS: *nematode-derived modular metabolites, peroxisomal β-oxidation, N-acyl ethanolamine, endocannabinoid signaling, lipogenesis*

INTRODUCTION

Lipophilic long-chain *N*-acyl ethanolamines (**1**, NAEs) constitute conserved lipid signaling molecules in plants, animals, and microorganisms (Figure 1a).[1−4] Polyunsaturated *N*-acyl ethanolamines (**1**) like anandamide (NAE-20:4 $\Delta^{5,8,11,14}$) and *N*-eicosapentaenoyl ethanolamine (NAE-20:5 $\Delta^{5,8,11,14,17}$), as well as related NAEs with *N*-oleoyl (18:1 Δ^{9}), *N*-linoleoyl (18:2 $\Delta^{9,12}$), *N*-*α*-linolenoyl (18:3 $\Delta^{9,12,15}$), or *N*-palmitoyl (16:0) residues (Figure 1c) function as endogenous ligands at G-protein-coupled receptors (CB1, CB2, GPR55, GPR110, GPR119),[5,6] ion channels (TRPV1),[7,8] and nuclear receptors (PPAR*α*).[8,9] Biogenesis of *N*-acyl ethanolamines (**1**) is initiated by *N*-acylation of membrane forming phosphatidylethanolamines (PEs, **3**), and the resulting *N*-acyl phosphatidylethanolamines (NAPEs, **5**) are converted into NAEs (**1**) via different pathways that include (a) direct cleavage by NAPE-specific phospholipase D (NAPE-PLD), (b) cleavage to *O*,*O*-diacyl glycerols (DAG) and *N*-acyl phosphoethanolamines (NAE-P, **2**) by phospholipase C (PLC), or (c) sequential cleavage via the corresponding *lyso*-NAPE (**6**) intermediates by *β*-hydrolase 4 (ABHD4) and *lyso*-NAPE-specific phospholipase D[10−16] (Figure 1a). NAE abundance is further regulated via their hydrolysis by fatty acid amide hydrolases (FAAH).[17,18]

The bacterivorous nematode *Caenorhabditis elegans* serves as a model organism to study lipogenesis and lipid metabolism, and their effect on lifespan and development.[19,20] Long-chain *N*-acyl ethanolamines (**1**), including NAE-20:4 and NAE-20:5, have previously been identified in *C. elegans*[21−23] and shown to

Received: January 20, 2025
Revised: April 29, 2025
Accepted: April 29, 2025
Published: June 30, 2025

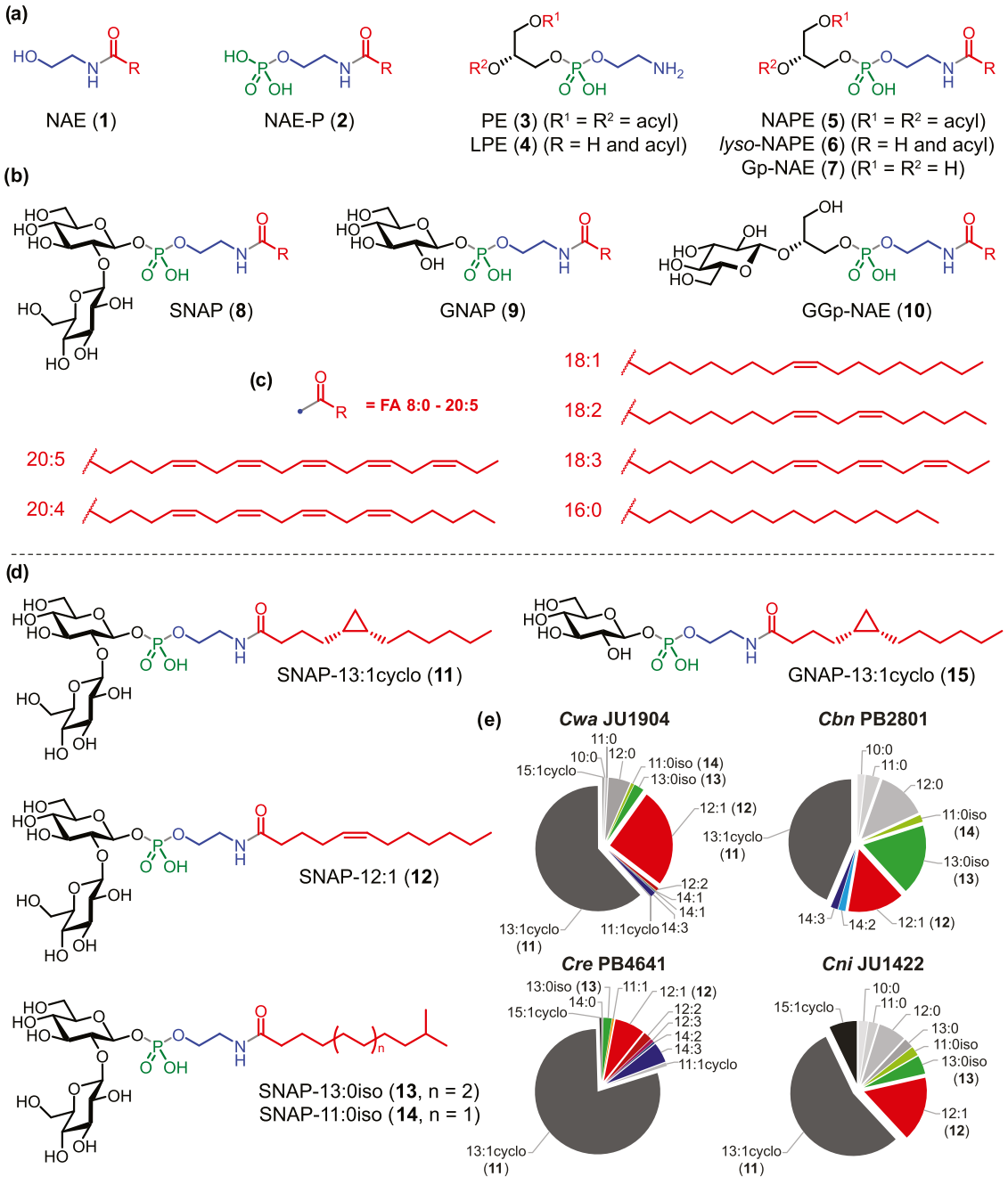

Figure 1. (a) Homologous *N*-acyl ethanolamines (NAEs, **1**) derived from *N*-acylation of phosphatidylethanolamines (**3**) via *N*-acyl phosphatidylethanolamines (NAPEs, **5**), either directly or via *N*-acyl phosphoethanolamine (**2**) or *lyso*-*N*-acyl phosphatidylethanolamine (*lyso*-NAPE, **6**) and *N*-acyl glycerylphosphoethanolamine (Gp-NAE, **7**) intermediates; (b) nematode-derived modular metabolites carrying homologous *N*-acyl ethanolamines building blocks: *β*-sophorosyl *N*-acyl phosphoethanolamines (**8**, SNAP), *β*-glucosyl *N*-acyl phosphoethanolamines (**9**, GNAP), and 2-(*β*-glucosyl)glyceryl *N*-acyl phosphoethanolamines (**10**, GGp-NAE); (c) Long-chain *N*-acyl residues of NAEs (**1**) involved in endocannabinoid signaling; (**d**) modular metabolites (**11**−**15**) isolated from *Caenorhabditis wallacei* JU1904 with *N*-acyl building blocks derived from peroxisomal *β*-oxidation; (**e**) Distribution of *β*-sophorosyl *N*-acyl phosphoethanolamines (**8**) in gonochoristic *C. wallacei* JU1904, *Caenorhabditis brenneri* PB2801, *Caenorhabditis remanei* PB4641, and *Caenorhabditis nigoni* JU1422.

modulate thermal avoidance,[24] olfactory sensitivity,[25] and cholesterol homeostasis[26] and coordinate nutrient status with metabolic changes that ultimately determine lifespan.[27−29] Two functional NAPE-PLD orthologues have been identified[30] along with NAE sensing G protein-coupled receptors such as NPR-19 and NPR-32.[31]

Biosynthesis of NAE-20:5 and NAE-20:4 (**1**) and related compounds is reduced in peroxisomal *β*-oxidation mutants such as *daf-22* (3-ketoacyl-*S*-CoA thiolase), presumably due to depletion of ethanolamine pools upon accumulation of copious amounts of ethanolamine conjugates of very long-chain ascarosides, the precursors of a conserved class of nematode signaling molecules.[32,33] Other peroxisomal *β*-oxidation mutants such as *acox-1* (acyl-CoA oxidase) exhibit no effect on NAE-20:5 and NAE-20:4 biosynthesis[32] but display a strongly reduced abundance of *lyso*-NAPEs (**6**) potentially involved in NAE biosynthesis.[34] While these results demonstrate the implication of peroxisomal *β*-oxidation in *C. elegans*'

https://doi.org/10.1021/acsbiomedchemau.5c00012
ACS Bio Med Chem Au 2025, 5, 602−619

NAE biosynthesis, the relationship between lipogenesis, β-oxidation, and NAE biogenesis has remained largely enigmatic.

Here, we demonstrate that *N*-acyl ethanolamine metabolisms in various *Caenorhabditis* spp., including the hermaphroditic model organism *C. elegans* as well as the gonochoristic *C. wallacei* and *C. brenneri*, involve multiple homologous series of fatty acid building blocks that either originate directly from the bacterial food source and the elongation of food-derived precursors or from de novo lipogenesis. A diversity of *N*-acyl units of medium chain length are derived from chain shortening of long-chain precursors via the *daf-22*-dependent peroxisomal β-oxidation cycle. Lipophilic *N*-acyl ethanolamines serve as building blocks for amphiphilic β-glycosyl *N*-acyl phosphoethanolamines (**8**, **9**) and 2-(β-glucosyl)-glyceryl *N*-acyl phosphoethanolamines (**10**) that are subsequently released into the environment, indicating potential signaling functions (Figure 1b). For example, the male-specific β-sophorosyl *N*-*cis*-5,6-methylenedodecanoyl phosphoethanolamine (**11**), which encodes the availability and growth phase of the *Escherichia coli* bacterial food source, retains females of *C. wallacei* and *C. brenneri*. Our results demonstrate that *N*-acyl ethanolamine metabolism is not only involved in endogenous signaling but also participates in intraspecies and potentially even interspecies interactions via amphiphilic signaling molecules released into the environment.

RESULTS

Identification of β-Sophorosyl *N*-Acyl Phosphoethanolamines from *C. wallacei*

Comparative ultrahigh-performance liquid chromatography electrospray ionization high-resolution tandem mass spectrometry (UHPLC-ESI-HR-MS^E) analysis of exometabolome extracts from seven *Caenorhabditis* species of the Elegans group, *C. elegans* N2, *C. brenneri* PB2801, *Caenorhabditis briggsae* AF16, *C. nigoni* JU1422, *C. remanei* PB4641, *Caenorhabditis tropicalis* JU1373, and *C. wallacei* JU1904 (Figure S1) highlighted a novel class of nematode-derived modular metabolites (NDMMs) that carry homologous *N*-acyl ethanolamine building blocks. Inspection of HR-MS/MS spectra (Figure S2) suggested modular β-glycosyl *N*-acyl phosphoethanolamine structures that integrate building blocks from carbohydrate, *N*-acyl ethanolamine, and energy metabolism. Two dominating representatives (**11** and **12**) were found to be particularly abundant in the exometabolome of the tropical species *C. wallacei* (previously called *C. sp. 16*) strain JU1904 from Central Bali, Indonesia,[35] and were subsequently isolated from 2 L of the liquid culture supernatant using a combination of reverse phase chromatography and semi-preparative high-performance liquid chromatography on RP-C18. Partial structures were identified by analysis of ^{1}H NMR, *dqf*-COSY, and HSQC spectra (Table S1), which indicated the presence of two β-glucopyranosyl units along with an ethanolamine moiety, whereas the variable *N*-acyl building blocks were identified as a cyclopropyl group containing *cis*-5,6-methylenedodecanoyl unit (13:1cyclo ($\Delta^{5,6}$)) or a monounsaturated (5*Z*)-dodecenoyl unit (12:1 (Δ^5)) for **11** and **12**, respectively (Figure 1d). The absolute configuration of the (5*R*,6*S*)-*cis*-cyclopropyl moiety of **11** was subsequently assigned based on its biosynthetic origin from *E. coli*-derived (9*R*,10*S*)-*cis*-9,10-methylenehexadecanoic acid (Figure S3) of known absolute configuration.[36] The characteristic disaccharide building block was identified as a β-sophorose (1,2-β-glucopyranosyl-glucopyranoside) unit based on long-range HMBC correlations (Figure S4). The connectivity of the modular building blocks as deduced from the HR-MS/MS fragmentation patterns (Figures S2 and S5) was finally confirmed by long-range H,H-COSY and H,C-HMBC correlations to reveal β-Sophorosyl *N*-Acyl Phosphoethanolamine (SNAP) structures that we like to call SNAP-13:1cyclo (**11**) and SNAP-12:1 (**12**). The energy-rich and rather labile β-sophorosyl-1-phosphate linkage was unambiguously established based on the vicinal ^3J-(H,P)-coupling constant of 8.8 Hz observed for an anomeric proton signal with *dd* multiplicity (Figure S6). The β-glycosyl-1-phosphate linkage in SNAP-13:1cyclo (**11**) and SNAP-12:1 (**12**) is prone to hydrolysis to furnish the corresponding *N*-acyl phosphoethanolamines (**2**) (Figure S7).

β-Glycosyl *N*-Acyl Phosphoethanolamines are Conserved in *Caenorhabditis* spp.

Having identified the two dominating β-sophorosyl *N*-acyl phosphoethanolamines from *C. wallacei* as SNAP-13:1cyclo (**11**) and SNAP-12:1 (**12**), we utilized their common characteristic ESI-(−)-HR-MS/MS fragment ion signal at *m*/*z* 78.9591 $[PO_3]^-$ for the phosphate unit to screen for additional minor derivatives (Figure S8). These analyses confirmed that SNAP-13:1cyclo (**11**) and SNAP-12:1 (**12**) are representatives of a diverse class of β-sophorosyl *N*-acyl phosphoethanolamines that share a common fragment ion of low intensity at *m*/*z* 421.0753 $[C_{12}H_{22}O_{14}P]^-$ for the β-sophorose-1-phosphate unit and carry homologues *N*-acyl residues of medium chain lengths ranging from 10 to 15 carbons (see Table S3 for 17 assigned structures). Comparative analysis of their chromatographic retention times indicated two homologous series with saturated straight chains or iso-branched *N*-acyl residues (Figure S9). Identification of the straight chain series was confirmed by chemical correlation of saturated SNAP-12:0 with SNAP-12:1 (**12**) using palladium-catalyzed hydrogenation (Figure S10). The assignment of iso-branched *N*-iso-acyl chains was subsequently confirmed by one and two-dimensional ^{1}H NMR spectroscopy of SNAP-13:0iso (**13**) and SNAP-11:0iso (**14**) isolated from *C. wallacei* JU1904 and *C. brenneri* PB2801 (Figure 1d and Table S1). Furthermore, using microreactions with palladium-catalyzed hydrogenation, a series of (odd-numbered) inert cyclopropyl group containing homologues were distinguished from the (even-numbered) double bond containing derivatives that are readily hydrogenated (Figure S11).

In addition, HR-MS/MS screening for *m*/*z* 78.9591 $[PO_3]^-$ (Figure S8) revealed a second series of closely related minor derivatives that are characterized by a monosaccharide building block instead of the β-sophorose unit (see Table S4). Analysis of HR-MS/MS (Figure S12) and one and two-dimensional ^{1}H NMR spectra (Figures S13 and 14) of isolated GNAP-13:1cyclo (**15**) (Figure 1d) as a representative for these β-Glucosyl *N*-Acyl Phosphoethanolamines (GNAP, **9**) confirmed the presence of a β-glucose-1-phosphate moiety (Table S1). Targeted screening of MS^E chromatograms for the β-glucose-1-phosphate fragment ion at *m*/*z* 259.0224 $[C_6H_{12}O_9P]^-$ demonstrated that the β-glucosyl *N*-acyl phosphoethanolamines (**9**) represent a diverse class of metabolites that carry homologous *N*-acyl moieties ranging from 7 to 20 carbons, including saturated straight and iso-branched building blocks, as well as cyclopropyl group containing and mono and polyunsaturated *N*-acyl units (see

https://doi.org/10.1021/acsbiomedchemau.5c00012
ACS Bio Med Chem Au 2025, 5, 602−619

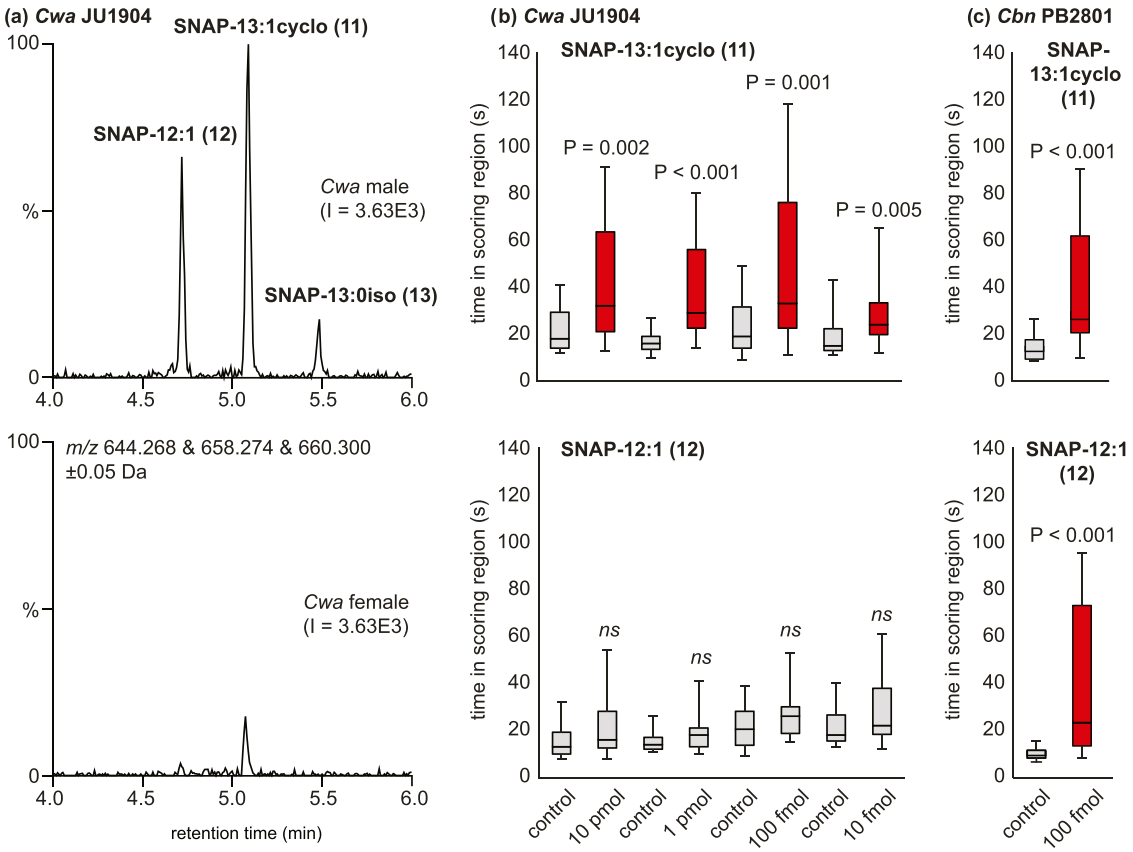

Figure 2. (a) Sex-specific analysis of *C. wallacei* JU1904 indicated that the dominating *β*-sophorosyl *N*-acyl phosphoethanolamines SNAP-13:1cyclo (**11**), SNAP-12:1 (**12**), and SNAP-13:0iso (**13**) are exclusively produced by males; (b) holding assays demonstrate that females of *C. wallacei* JU1904 are retained in scoring regions conditioned with male-produced SNAP-13:1cyclo (**11**) but not with SNAP-12:1 (**12**), whereas (c) females of *C. brenneri* PB2801 are retained by both SNAP-13:1cyclo (**11**) and SNAP-12:1 (**12**) (Welch's *t* test, *ns* = not significant, see Tables S9 and S10 for data).

Table S4 for 46 assigned structures, some of which have been previously detected[23]). Comparative UHPLC-ESI-HR-MS^E analysis of exometabolome extracts of seven *Caenorhabditis* species from the Elegans group revealed that modular *β*-glycosyl *N*-acyl phosphoethanolamines (**8** & **9**) are highly conserved. The gonochoristic species represented by *C. wallacei*, *C. brenneri*, *C. nigoni*, and *C. remanei* produce predominantly *β*-sophorosyl *N*-acyl phosphoethanolamines (**8**) with SNAP-13:1cyclo (**11**) as the dominating component in all four species (Figure 1e) along with a diversity of species-specific minor *β*-glycosyl *N*-acyl phosphoethanolamines (**8** & **9**). In contrast, all three androdiecious *Caenorhabditis* species described so far, *C. elegans*, *C. briggsae*, and *C. tropicalis* were found to produce only traces of the *β*-sophorosyl *N*-acyl phosphoethanolamines (SNAP, **8**) but instead release the corresponding *β*-glucosides (GNAP, **9**). The *β*-glycosyl *N*-acyl phosphoethanolamine profile of the model organism *C. elegans* N2 is dominated by compounds containing *N*-cyclopropyl-acyl moieties like 11:1cyclo, 13:1cyclo, and 15:1cyclo moieties, as well as the polyunsaturated *N*-eicosapentaenoyl moiety (20:5), along with minor amounts of straight and iso-branched-chain derivatives (Figure 6f).

Male-Produced *β*-Sophorosyl *N*-Acyl Phosphoethanolamines Attract Females

Sex-specific exometabolome analysis of gonochoristic *C. wallacei* JU1904 demonstrated that the three representative *β*-sophorosyl *N*-acyl phosphoethanolamines SNAP-13:1cyclo (**11**), SNAP-12:1 (**12**), and SNAP-13:0iso (**13**) are predominantly produced by males (Figure 2a). Male-specific production of SNAP-13:1cyclo (**11**), SNAP-12:1 (**12**), and SNAP-13:0iso (**13**) was also demonstrated for gonochoristic *C. brenneri* PB2801, *C. nigoni* JU1422, and *C. remanei* PB4641 (Figure S15). In addition, male specificity could also be demonstrated for most of the minor *β*-sophorosyl *N*-acyl phosphoethanolamines (**8**) carrying straight chain, iso-branched, unsaturated, and cyclopropyl groups containing *N*-acyl residues (Figure S16). In contrast, the corresponding monosaccharides such as GNAP-13:1cyclo (**15**) were detected in males and females of the gonochoristic *Caenorhabditis* species and even appeared to be somewhat enriched in females (Figure S17). These *β*-glucosyl *N*-acyl phosphoethanolamines (**9**) are abundant in androdiecious *C. elegans*, *C. briggsae*, and *C. tropicalis*. Their production in *C. elegans* is largely unaffected by the *him-5(e1490)* mutation (Figure S18) that is characterized by a high incidence of males, approximately 33% versus 0.3% for the N2 wild type,[37] which confirms that *β*-glucosyl *N*-acyl phosphoethanolamines (**9**) such as GNAP-13:1cyclo (**15**) are predominantly produced by hermaphrodites.

The biological activity of male-produced SNAP-13:1cyclo (**11**) and SNAP-12:1 (**12**) on *C. wallacei* adult behavior was evaluated using a holding assay that quantifies nematode retention in conditioned scoring regions in comparison to the solvent control (Table S9). Whereas males are not affected, females are retained by ecologically relevant amounts of

https://doi.org/10.1021/acsbiomedchemau.5c00012
ACS Bio Med Chem Au 2025, 5, 602−619

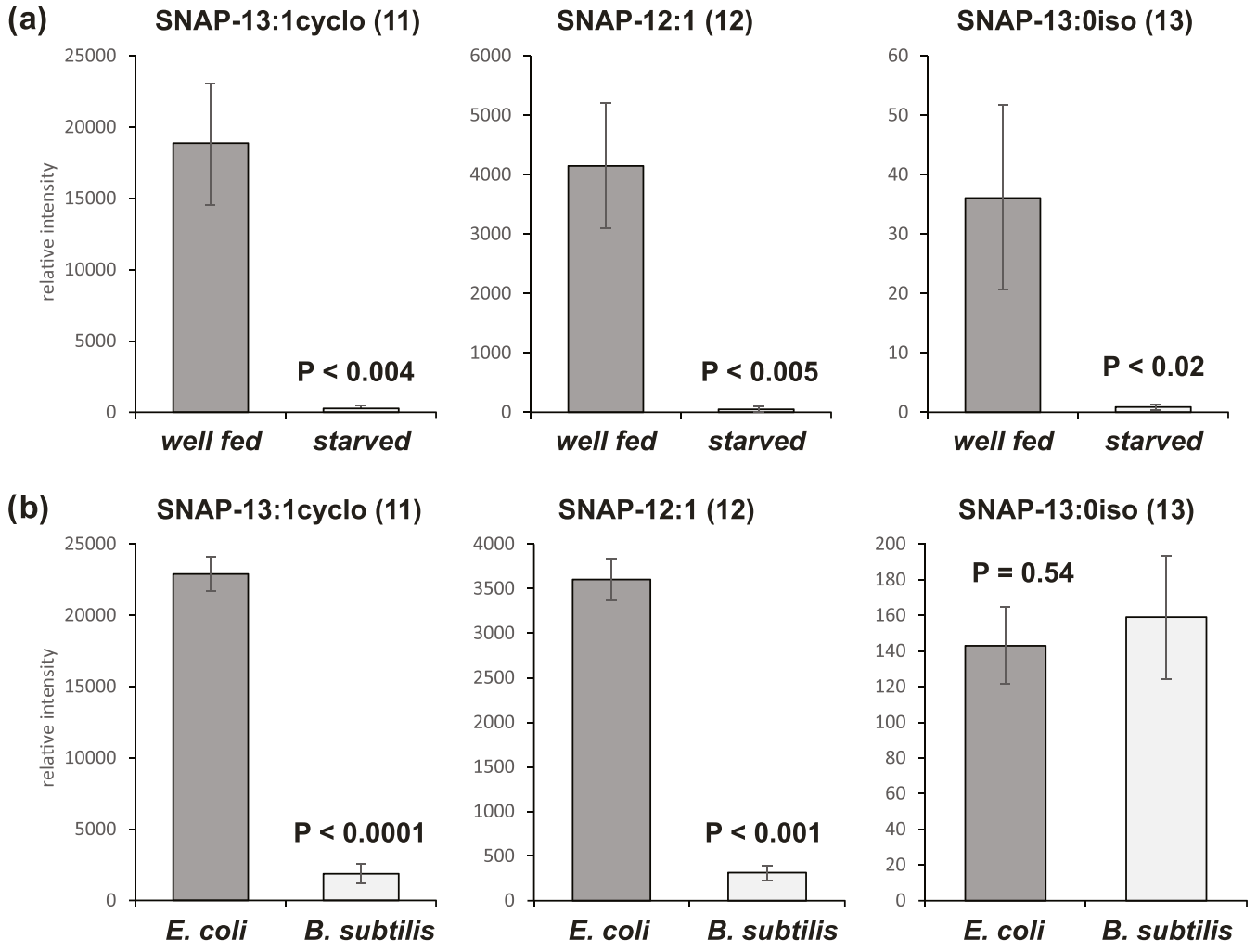

Figure 3. Food-dependent biosynthesis of *β*-sophorosyl *N*-acyl phosphoethanolamine (SNAP) in *C. wallacei* JU1904. (a) Biosynthesis of SNAP-13:1cyclo (**11**) SNAP-12:1 (**12**), and SNAP-13:0iso (**13**) subsides upon starvation (relative intensity, mean ± 1 SD, $n = 4$); (b) Biosynthesis of SNAP-13:1cyclo (**11**) and SNAP-12:1 (**12**) strongly depends on the *E. coli* diet, whereas that of SNAP-13:0iso (**13**) is independent of the bacterial food source (relative intensity, mean ± 1 SD; Welch's *t* test, $n = 3$).

SNAP-13:1cyclo (**11**) ranging from 10 fmol to 10 pmol (Figure 2b). In contrast, SNAP-12:1 (**12**) did not elicit any significant response in males or females at any of the concentrations tested, which demonstrates that the presence of the cyclopropyl moiety is essential for the behavioral activity of SNAP-13:1cyclo (**11**) in *C. wallacei* females. Females of *C. brenneri* are retained by 100 fmol of both SNAP-13:1cyclo (**11**) or SNAP-12:1 (**12**) (Figure 2c), although male production of SNAP-13:1cyclo (**11**) is considerably more pronounced than those of SNAP-12:1 (**12**) (Figure S15). *C. brenneri* males did not respond to any of the compounds tested (Table S10).

Biogenesis of *β*-Sophorosyl *N*-Acyl Phosphoethanolamines Depends on Bacterial Food Availability

To decipher the ecological significance of female retention by male-produced SNAP-13:1cyclo (**11**), the biogenesis of the *β*-glycosyl *N*-acyl phosphoethanolamines was investigated. Bacterial food dependency was evaluated by comparative UHPLC-HR-MS analysis of the conditioned media supernatant collected from well-fed versus starved *C. wallacei* cultures, which demonstrates that SNAP-13:1cyclo (**11**), SNAP-12:1 (**12**), and SNAP-13:0iso (**13**) accumulate under well-fed conditions, whereas their production is largely abolished upon starvation (Figure 3a). Similar results were obtained for a diversity of homologous *β*-glycosyl *N*-acyl phosphoethanolamines (**8**, **9**) in *C. wallacei* and *C. brenneri* (Figures S19 and S20). This pronounced food dependency resembles those observed for the dominating 1- and 2-isomeric *lyso*-phosphatidylethanolamines (LPEs, **4**) with homologous long-chain *O*-acyl side chains such as 14:0, 16:0, 18:0, 16:1, 18:1, 17:1cyclo, and 19:1cyclo (Figure S21 and Table S5) that are derived from partial hydrolysis of bacterial membrane forming phosphatidylethanolamines (PEs, **3**). In contrast, the biosynthesis of ascarosides, a class of conserved nematode glycolipids with diverse signaling functions,[38,39] is largely maintained when shifting from well-fed to starved conditions (Figure S22), suggesting that their fatty acid-derived aglycones originate from stored lipid reservoirs (or de novo lipogenesis), whereas the fatty acid moieties of the *β*-glycosyl *N*-acyl phosphoethanolamines (**8**, **9**) are more directly derived from the bacterial diet.

Time-dependent quantitative analysis based on the comparison of released versus retained metabolites, the exo- and endometabolome, respectively, indicated that under well-fed conditions, approximately 5-20% of SNAP-13:1cyclo (**11**) and

https://doi.org/10.1021/acsbiomedchemau.5c00012
ACS Bio Med Chem Au 2025, 5, 602−619

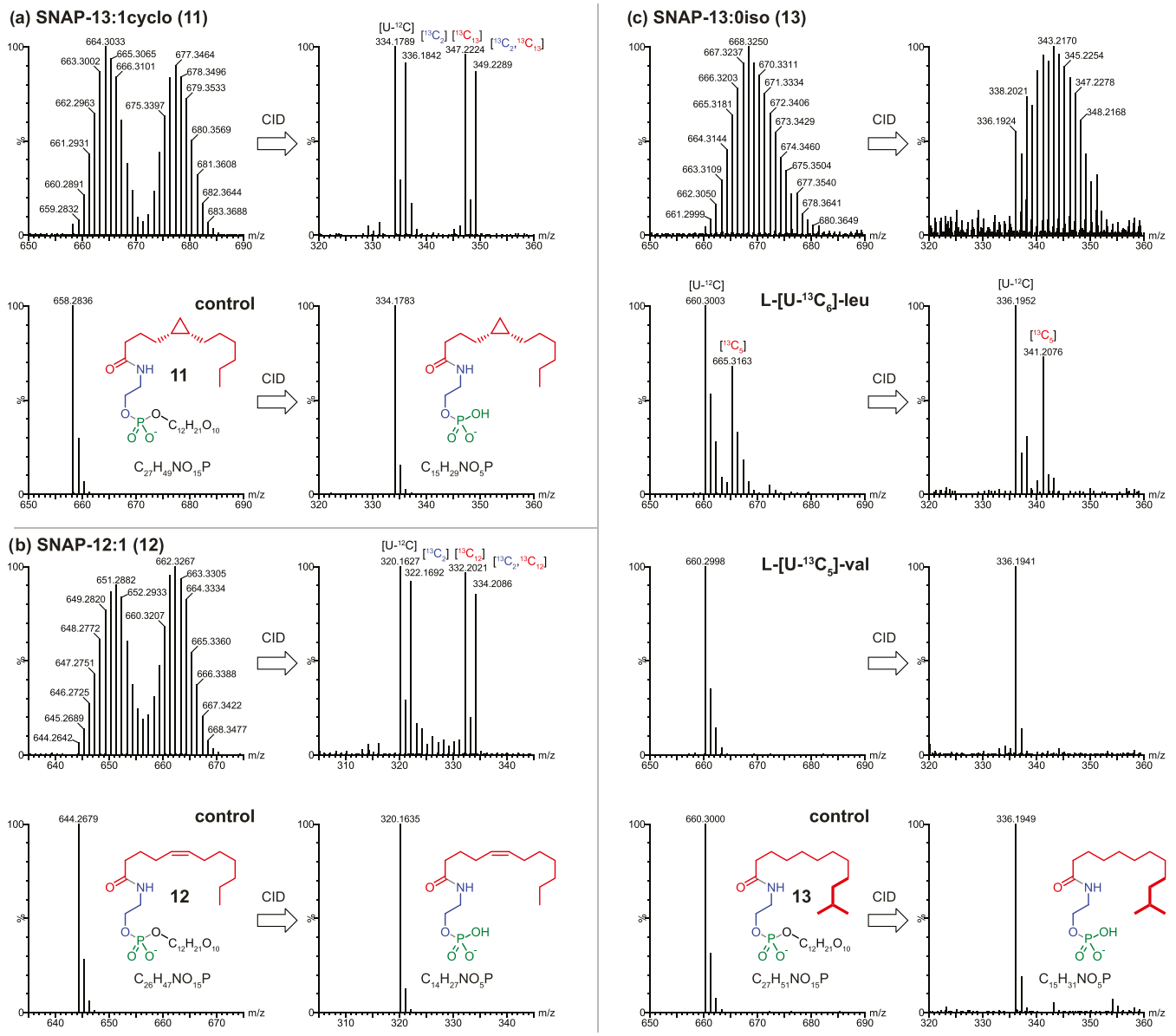

Figure 4. ESI-(−)-HR-MS^E spectra showing the distribution of ^{13}C isotopomers for molecular ions $[M - H]^-$ and CID-derived *N*-acyl phosphoethanolamine fragment ions $[M - C_{12}H_{21}O_{10}]^-$ of SNAP-13:1cyclo (**11**), SNAP-12:1 (**12**), and SNAP-13:0iso (**13**) upon mixed isotope labeling by feeding *C. wallacei* JU1904 with a 1:1 mixture of [U−^{12}C]- and [U−^{13}C]-*E. coli*, along with natural abundance spectra as control. (a, b) Biogenesis of SNAP-13:1cyclo (**11**) and SNAP-12:1 (**12**) depends on the assembly of bacteria-derived *N*-acyl and ethanolamine units along with a sophorose unit from gluconeogenesis. (c) In contrast, SNAP-13:1iso (**13**) depends on de novo lipogenesis of the *N*-iso-acyl moiety, which incorporates a [$^{13}C_5$]-isovalerate building block upon feeding with 50% L-[U−$^{13}C_6$]-leucine enriched *E. coli*, but is not labeled by L-[U−$^{13}C_5$]-valine.

SNAP-12:1 (**12**) present in worm bodies is being released into the environment every hour (Figure S23), which is comparable to the release rates observed for most ascaroside signals (asc-C5-C9:10-40%/h) but considerably lower than those observed for the dominating LPEs (**4**) derived from direct hydrolysis of *E. coli* PEs (e.g., LPE-14:0, LPE-16:0, LPE-17:1cyclo, LPE-19:1cyclo with 80-160%/h). Starved nematodes retain only limited reservoirs of SNAP-13:1cyclo (**11**, 9% of well-fed), SNAP-12:1 (**12**, 26%), or SNAP-13:0iso (**13**, 16%) (Figure S24), suggesting that the *β*-sophorosyl *N*-acyl phosphoethanolamines represent (slowly) released environmental signals that potentially serve as a measure for food availability.

Assembly of *β*-Sophorosyl *N*-Acyl Phosphoethanolamines Combines Bacterial Lipogenesis and Nematode Gluconeogenesis

Aiming to decipher the biosynthetic origin of the *β*-sophorosyl *N*-acyl phosphoethanolamines, we utilized the mixed [U−^{12}C]/[U−^{13}C]-isotope labeling strategy,[40−42] in order to discriminate food-derived and de novo biosynthesized metabolic building blocks. After feeding *C. wallacei* with a 1:1 mixture of natural abundance [U−^{12}C] and uniformly carbon-13 labeled [U−^{13}C]-*E. coli*, the exometabolome extract was fractionated by RP-C18 chromatography to enrich the target compounds. Analysis of ESI-(−)-HR-MS^E spectra revealed a bimodal distribution of ^{13}C isotopomers for the molecular ion signal of SNAP-13:1cyclo (**11**), whereas the

https://doi.org/10.1021/acsbiomedchemau.5c00012
ACS Bio Med Chem Au 2025, 5, 602−619

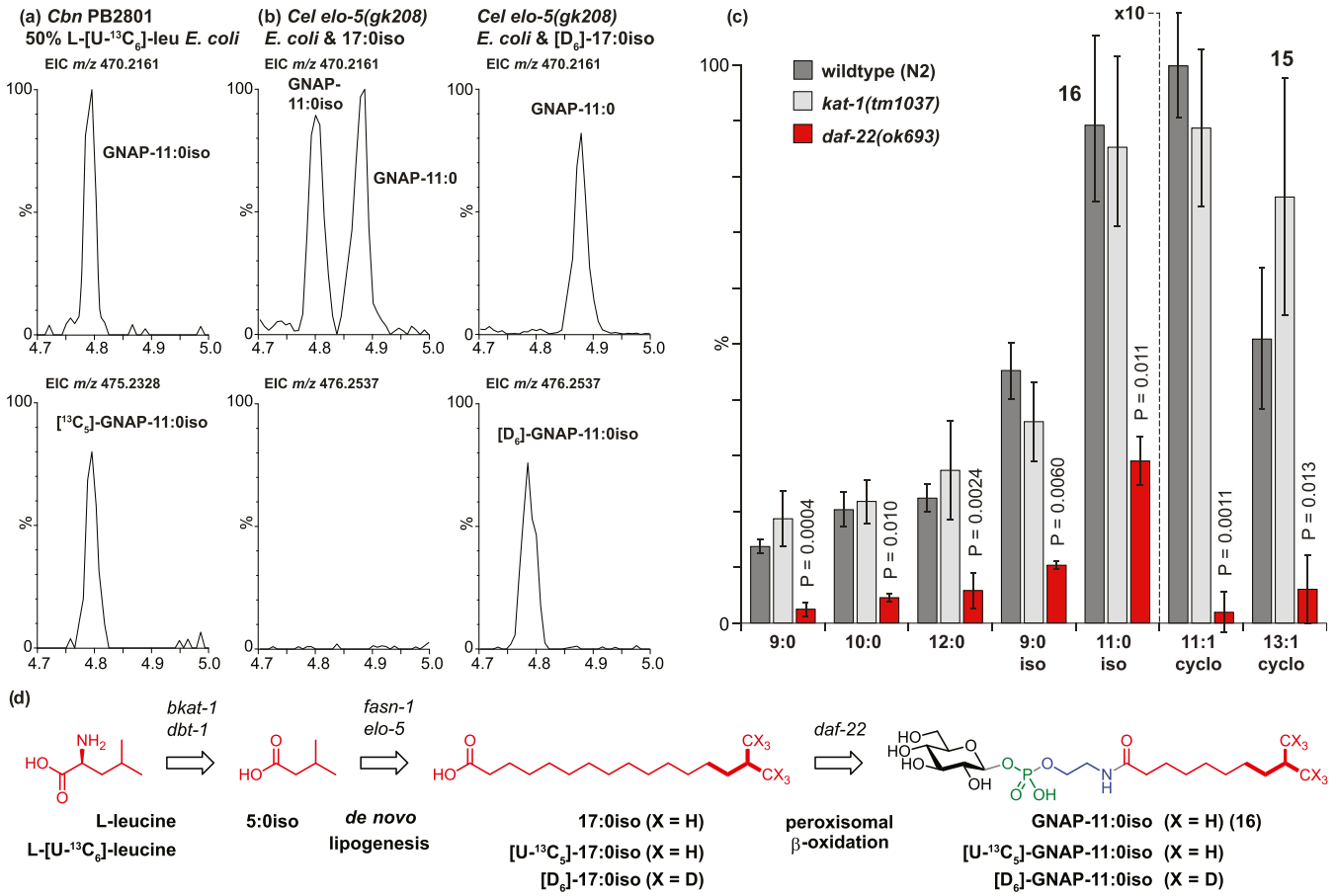

Figure 5. (a) Incorporation of L-[U−$^{13}C_6$]-leucine labeled *E. coli* (50% enrichment) into [$^{13}C_5$]-GNAP-11:0iso ([$^{13}C_5$]-**16**) in *C. brenneri* PB2801; (b) incorporation of natural abundance 17:0iso or [D_6]-17:0iso by *C. elegans elo-5(gk208)* provides exclusively GNAP-11:0iso (**16**) or [D_6]-GNAP-11:0iso ([D_6]-**16**), respectively; (c) comparative UHPLC-ESI-(−)-HR-MS analysis of *C. elegans* wild-type (N2) and *β*-oxidation mutant exometabolomes reveals that *β*-glycosyl *N*-acyl ethanolamine phosphate (GNAP) biosynthesis is independent of the mitochondrial 3-ketoacyl-*S*-CoA thiolase *kat-1* but proceeds via the peroxisomal 3-ketoacyl-*S*-CoA thiolase *daf-22* (relative intensity, mean ± 1 SD, n = 3); and (d) biosynthetic pathway from L-leucine to GNAP-11:0iso (**16**) via *elo-5*-dependent de novo lipogenesis of iso-fatty acids such as 17:0iso and subsequent chain shortening via peroxisomal *β*-oxidation by *daf-22*.

corresponding 13:1cyclo ($\Delta^{5,6}$) *N*-acyl phosphoethanolamine (**2**) fragment ion from loss of the *β*-sophorose unit shows discrete signals for [U−^{12}C], [$^{13}C_2$], [$^{13}C_{13}$], and [U−$^{13}C_{15}$] isotopomers (Figures 4a and S25), which demonstrates that SNAP-13:1cyclo (**11**) is produced by the nematode upon combining a [C_{13}]-13:1cyclo fatty acid and a [C_2]-ethanolamine building block derived from bacterial metabolism, along with two glucose units derived from de novo gluconeogenesis. A similar bimodal ^{13}C isotopomer distribution was observed for SNAP-12:1 (**12**) along with discrete signals for [U−^{12}C], [$^{13}C_2$], [$^{13}C_{12}$], and [U−$^{13}C_{14}$] isotopomers for the monounsaturated 12:1 (Δ^5) *N*-acyl phosphoethanolamine fragment ion (**2**) (Figures 4b and S25), indicating its origin from the bacterial diet. However, minor signals for ^{13}C isotopomers with a bell shape distribution also suggested some incorporation of de novo biosynthesized 16:1 (Δ^9) or 18:1 (Δ^{11}).[40] The bacterial origin of both 12:1 (Δ^5) and 13:1cyclo ($\Delta^{5,6}$) *N*-acyl units and the ethanolamine building block along with their assembly by the nematode could also be confirmed for [C_{13},C_2]-NAE-P-13:1cyclo and [C_{12},C_2]-NAEP-12:1, the corresponding *N*-acyl phosphoethanolamines (**2**) (Figure S26) derived from hydrolysis of SNAP-13:1cyclo (**11**) and SNAP-12:1 (**12**), respectively (Figure S7).

Biogenesis of *β*-Sophorosyl *N*-Acyl Phosphoethanolamines Depends on the Bacterial Diet

In order to explore how the lipid composition of the bacterial diet affects the biosynthesis of *β*-sophorosyl *N*-acyl phosphoethanolamines, *C. wallacei* was cultivated with either the standard *E. coli* OP50 diet or with *Bacillus subtilis*, an alternative food source that has been shown to affect nematode reproduction, fitness, and lifespan.[43] Characterization of the fatty acid composition of the *E. coli* OP50 lipidome using fatty acid methyl ester (FAME) analysis by GC-EIMS showed two cyclopropyl fatty acids, 17:1cyclo ($\Delta^{9,10}$) and 19:1cyclo ($\Delta^{11,12}$), along with monounsaturated palmitoleic acid (16:1 (Δ^9)) and *cis*-vaccenic acid (18:1 (Δ^{11})) (Figure S27a), which represent potential precursors for the *N*-acyl units of SNAP-13:1cyclo ($\Delta^{5,6}$) (**11**) and SNAP-12:1 (Δ^5) (**12**), respectively. In contrast, the lipidome of *B. subtilis* is characterized by the absence of cyclopropyl and monounsaturated fatty acids and instead represents a rich source of iso- and anteiso-fatty acids such as 15:0iso, 17:0iso, 15:0anteiso, and 17:0anteiso (Figure S27b).[44] Shifting *C. wallacei*'s diet from *E. coli* to *B. subtilis* resulted in specific and strong attenuation of SNAP-13:1cyclo (**11**) and SNAP-12:1 (**12**) (Figure 3b), which indicates that their production depends on the bacterial diet and requires bacterial cyclopropyl and monounsaturated fatty acids,

https://doi.org/10.1021/acsbiomedchemau.5c00012
ACS Bio Med Chem Au 2025, 5, 602−619

respectively. Bacterial food-dependent biosynthesis was also observed for GNAP-13:1cyclo (**15**) (Figure S28), a dominating β-glycosyl *N*-acyl phosphoethanolamine in the model organism *C. elegans*. In contrast, branched-chain β-sophorosyl *N*-iso-acyl phosphoethanolamines such as SNAP-13:0iso (**13**) are not affected by shifting from *E. coli* to an iso-fatty acid rich *B. subtilis* diet (Figure 3b). These results indicate that the bacterivorous nematode *C. wallacei* requires *E. coli*-derived cyclopropyl fatty acids (17:1cyclo ($\Delta^{9,10}$) and 19:1cyclo ($\Delta^{11,12}$)) and their monounsaturated precursors, palmitoleic (16:1 (Δ^{9})) and *cis*-vaccenic acid (18:1 (Δ^{11})) for biosynthesis of SNAP-13:1cyclo (**11**) and SNAP-12:1 (**12**), respectively, which further implies chain shortening of these long-chain fatty acids (potentially via β-oxidation) to produce the 13:1cyclo ($\Delta^{5,6}$) and 12:1 (Δ^{5}) *N*-acyl building blocks of SNAP-13:1cyclo (**11**) and SNAP-12:1 (**12**), respectively. Considering that *E. coli* represents an artificial food source for bacterivorous *Caenorhabditis* spp. and that bacterial fatty acid components are required for the biosynthesis of SNAP-13:1cyclo (**11**) and SNAP-12:1 (**12**), we screened the fatty acid composition of a set of 12 bacterial strains isolated from the *C. elegans* microbiome (the CeMBio collection[45]) by GC-EIMS (Figure S29), which demonstrated that both cyclopropyl fatty acid and palmitoleic acid are abundant lipid components in *Caenorhabditis'* natural environment.

Iso-Branched β-Glycosyl *N*-Iso-acyl Phosphoethanolamines Depend on De Novo Lipogenesis by *elo-5*

In contrast to the bacteria-derived *N*-acyl building blocks of SNAP-13:1cyclo (**11**) and SNAP-12:1 (**12**) (Figure 4a,b), mixed isotope labeling of SNAP-13:0iso (**13**) in *C. wallacei* using a 1:1 mixture of natural abundance [U−^{12}C]- and carbon-13 labeled [U−^{13}C]-*E. coli* (Figure 4c) furnished a bell-shaped distribution of ^{13}C isotopomers for the *N*-iso-tridecanoyl phosphoethanolamine fragment ion, indicating a de novo origin for the branched-chain *N*-iso-acyl moiety of SNAP-13:0iso (**13**). Production of iso-branched SNAP-13:0iso (**13**) in *C. wallacei* is independent of the iso-fatty acid content of the bacterial diet (Figure 3b), in agreement with a de novo origin. Feeding *C. brenneri* with an auxotrophic *E. coli* Δ*val*, Δ*leu*, Δ*ile* mutant specifically enriched with either 50% L-[U−$^{13}C_6$]-leucine or 50% L-[U−$^{13}C_5$]-valine revealed that iso-branched SNAP-13:0iso (**13**) (Figures 4c, and S30) and GNAP-11:0iso (**16**) (Figure 5a) are [$^{13}C_5$]-labeled upon incorporation of L-[U−$^{13}C_6$]-leucine but not by L-[U−$^{13}C_5$]-valine. Incorporation of L-[U−$^{13}C_6$]-leucine enriched *E. coli* also furnished [$^{13}C_5$]-labeled iso-fatty acids [$^{13}C_5$]-15:0iso and [$^{13}C_5$]-17:0iso (Figure S31), thus suggesting that the *N*-iso-acyl moiety of SNAP-13:0iso (**13**) and GNAP-11:0iso (**16**) might originate from de novo lipogenesis of odd-numbered iso-fatty acids, which represent essential building blocks for branched-chain d17:1iso sphingosine and related sphingolipids characteristic for nematodes.[46−49] De novo lipogenesis of iso-fatty acids involves the chain elongation of a L-leucine-derived isovalerate unit[50,51] and depends on the iso-fatty acid elongase *elo-5* that participates in the elongation of 13:0iso to 15:0iso.[49,52,53] Implication of *elo-5* in the biogenesis of the β-glucosyl *N*-iso-acyl phosphoethanolamine GNAP-11:0iso (**16**) was demonstrated using the *C. elegans elo-5(gk208)* loss of function mutant that is known to arrest larval development at the L1 stage unless supplemented with an exogenous source of iso-branched fatty acids such as 15:0iso or 17:0iso.[53] Comparative analysis of *elo-5(gk208)* cultures supplemented with either synthetic 17:0iso or its stable isotope labeled [D_6]-isotopomer[49,54] furnished exclusively natural abundance GNAP-11:0iso (**16**) or isotope labeled [D_6]-GNAP-11:0iso ([D_6]-**16**), respectively (Figure 5b), which not only demonstrated that GNAP-11:0iso (**16**) biogenesis in *C. elegans* depends on *elo-5* but also revealed that it proceeds exclusively via chain shortening of a long-chain iso-fatty acid intermediate such as 17:0iso and not directly via de novo lipogenesis of the medium-chain 11:0iso fatty acid building block (Figure 5d).

Biosynthesis of β-Glycosyl *N*-Acyl Phosphoethanolamines Depends on Peroxisomal β-Oxidation by *daf-22*

Considering that the biosynthesis of the various *N*-acyl building blocks of β-glycosyl *N*-acyl phosphoethanolamines in *Caenorhabditis* spp. appears to depend on chain shortening of long-chain fatty acids derived from either the bacterial diet or de novo lipogenesis, we screened *C. elegans* β-oxidation mutants carrying deletions in the peroxisomal 3-ketoacyl-*S*-CoA thiolase *daf-22*[55−57] or the mitochondrial 3-ketoacyl-*S*-CoA thiolase *kat-1*.[58] Comparative exometabolome analysis of *C. elegans* wild-type N2, *daf-22(ok693)*, and *kat-1(tm1037)* demonstrates that the biosynthesis of β-glucosyl *N*-acyl phosphoethanolamines does not require mitochondrial *kat-1* but depends on the peroxisomal β-oxidation cycle that involves *daf-22* (Figure 5c). Production of β-glycosyl *N*-acyl phosphoethanolamines in the *daf-22* mutant is strongly attenuated for straight chain and iso-branched derivatives like GNAP-11:0iso (**16**) and almost abolished for the cyclopropyl group containing GNAP-13:1cyclo (**15**). These results demonstrate that both β-glycosyl *N*-acyl phosphoethanolamine (Figure 5c) and ascaroside biosynthesis[59] depend on *daf-22* (Figure S32) and utilize the same primary metabolic pathway, the peroxisomal β-oxidation of long-chain fatty acids (LCFAs), to regulate the chain lengths of lipid-derived homologous acyl building blocks. However, while the *daf-22* mutant accumulates homologous long-chain ascarosides that represent the direct precursors for the short-chain components characteristic for the wild type (Figure S32),[59,60] no accumulation of any long-chain homologue was observed for the β-glycosyl *N*-acyl phosphoethanolamines, suggesting that the subsequent biosynthetic steps that connect peroxisomal β-oxidation and β-glycosyl *N*-acyl phosphoethanolamine biosynthesis are selective for specific medium-chain fatty acid (MCFAs) building blocks.

Characterization of *N*-Acyl Ethanolamines as Putative Biosynthetic Intermediates

Having shown that the biosynthesis of β-glycosyl *N*-acyl phosphoethanolamine (**8** and **9**) with medium-length *N*-acyl building blocks depends on peroxisomal β-oxidation of fatty acids, we aimed to characterize putative biosynthetic intermediates. Targeted ESI-(+)-HR-MS^E analysis by screening for $[C_2H_8NO]^+$ at *m*/*z* 62.061 (Figure S33) enabled the detection of previously described long-chain *N*-acyl ethanolamines (NAEs, **1**)[23,27−33] as part of a homologous series carrying *N*-acyl units ranging from 10 to 20 carbons (see Table S6 for 55 assigned structures) that are highly conserved in *Caenorhabditis* spp. NAE-15:1cyclo is dominating in *C. elegans* fed with *E. coli*, while the other androdiecious *Caenorhabditis* species produce predominantly NAE-20:5 (*C. briggsae*) or NAE-18:1 (*C. tropicalis*) (Figure S34). Biosynthesis of the homologous *N*-acyl chains in NAEs (**1**) parallels those of SNAPs (**8**) and GNAPs (**9**). De novo produced branched-

https://doi.org/10.1021/acsbiomedchemau.5c00012
ACS Bio Med Chem Au 2025, 5, 602−619

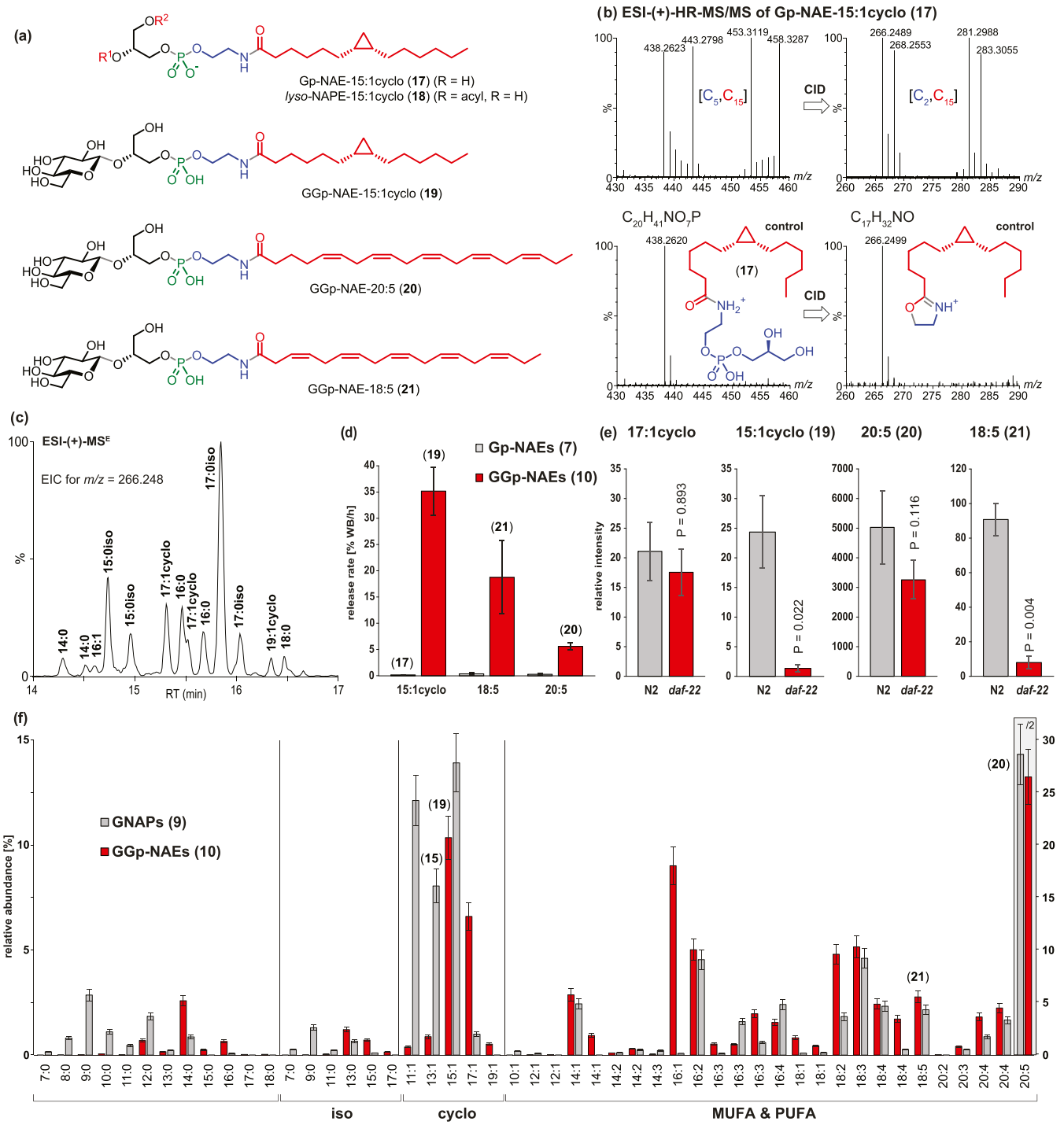

Figure 6. (a) Structures of *N*-acyl glycerylphosphoethanolamine (Gp-NAE-15:1cyclo, **17**) and the corresponding homologous series of *O*-acyl *N*-acyl glycerylphosphoethanolamines (*lyso*-NAPE-15:1cyclo, **18**), and the dominating *N*-acyl 2-(*β*-glucosyl)-glycerylphosphoethanolamines (GGp-NAEs, **19**−**21**) isolated from the *C. elegans* exometabolome; (b) ESI-(−)-HR-MS and MS^E spectra of Gp-NAE-15:1cyclo (**17**) showing the distribution of ^{13}C isotopomers for $[C_{15},C_5]$-Gp-NAE-15:1cyclo (**17**) as $[M-H]^-$ and dehydrated $[C_{15},C_2]$-NAE-15:1cyclo fragment ion upon mixed isotope labeling by feeding *C. wallacei* JU1904 with a 1:1 mixture of [U−^{12}C]- and [U−^{13}C]-*E. coli*, along with natural abundance spectra as control; (c) extracted ion chromatogram for *m*/*z* 266.248 for NAE-*cy*15:1 fragment ions reveals diverse *lyso*-NAPE-*cy*15:1 (**18**) with homologous 1,2-isomeric *O*-acyl building blocks; (d) while Gp-NAEs (**7**) are enriched in the endolipidome, their release rates drastically increase upon 2-*β*-glucosylation to the corresponding GGp-NAEs (**10**); (e) biosynthesis of GGp-NAE-15:1cyclo (**19**) and GGp-NAE-18:5 (**21**) is almost abolished in the *daf-22* metabolome, whereas those of GGp-NAE-17:1cyclo and GGp-NAE 20:5 (**20**) is only slightly reduced, demonstrating the implication of *daf-22*-dependent peroxisomal *β*-oxidation; and (f) composition of homologous *β*-glucosyl *N*-acyl phosphoethanolamines (GNAP, **9**) and *N*-acyl 2-(*β*-glucosyl)-glycerylphosphoethanolamines (GGp-NAE, **10**) in the *C. elegans* exometabolome.

chain *N*-iso-acyl ethanolamines incorporate a [$^{13}C_5$]-isovalerate unit upon feeding with L-[U−$^{13}C_6$]-leucine enriched *E. coli* (Table S6 and Figure S35). Production of long-chain polyunsaturated *N*-acyl ethanolamines is partially down-regulated in *daf-22* as previously reported,[32,33] whereas the biogenesis of several chain-shortened homologues, including

https://doi.org/10.1021/acsbiomedchemau.5c00012
ACS Bio Med Chem Au 2025, 5, 602−619

NAE-15:1cyclo, NAE-13:1cyclo, NAE-15:0iso, NAE-13:0iso, and NAE-18:5, is almost abolished in the *daf-22* mutant (Figure S36), demonstrating their origin from chain shortening of long-chain precursors via the peroxisomal β-oxidation cycle. Mixed isotope labeling by feeding *C. wallacei* with a 1:1 mixture of natural abundance [U−^{12}C]- and carbon-13 labeled [U−^{13}C]-*E. coli* afforded a diversity of [C_n,C_2]-labeled *N*-acyl ethanolamines (*n* = carbon number of *N*-acyl unit) such as [C_{16},C_2]-NAE-16:0, [C_{19},C_2]-NAE-19:1cyclo, [C_{17},C_2]-NAE-17:1cyclo, [C_{15},C_2]-NAE-15:1cyclo, and [C_{13},C_2]-NAE-13:1cyclo, as well as chain elongated homologues with polyunsaturated *N*-octadecanoyl or *N*-eicosanoyl moieties such as [C_{16},C_2,C_2]-NAE-18:X (X = 3-5), [C_{16},C_2,C_2,C_2]-NAE-20:4 (anandamide) and [C_{16},C_2,C_2,C_2]-NAE-20:5, along with de novo biosynthesized iso-branched derivatives such as NAE-15:0iso and NAE-17:0iso (Figure S37), which demonstrates that *N*-acyl ethanolamines are produced by the nematode via assembly of an ethanolamine unit with a diversity of homologous *N*-acyl building blocks derived from either bacterial lipogenesis, chain elongation of bacteria-derived palmitic acid (16:0), or de novo lipogenesis. Furthermore, identification of chain-shortened homologues, such as [C_{15},C_2]-NAE-15:1cyclo and [C_{13},C_2]-NAE-13:1cyclo (originating from *E. coli*-derived 17:1cyclo and 19:1cyclo) or [C_{16},C_2,C_2]-NAE-18:5 (originating from 20:5), and their *daf-22* dependence, demonstrates that *N*-acyl ethanolamine metabolism also incorporates building blocks derived from peroxisomal β-oxidation of long-chain fatty acid precursors.

Glyceryl *N*-Acyl Phosphoethanolamines (Gp-NAEs) are Putative Intermediates in β-Glycosyl *N*-Acyl Phosphoethanolamine Biosynthesis

Aiming to identify the biosynthetic intermediates that link *daf-22*-dependent peroxisomal β-oxidation of long-chain fatty acids with *N*-acyl ethanolamine metabolism and β-glycosyl *N*-acyl phosphoethanolamine biosynthesis, the exo- and endometabolomes of *Caenorhabditis* spp. were analyzed for modular metabolites that carry the characteristic *N*-acyl ethanolamine building blocks. Targeted ESI-(+)-HR-MS/MS screening revealed a limited collection of glyceryl *N*-acyl phosphoethanolamines (Gp-NAEs, **7**) with 11:1cyclo, 13:1cyclo, 15:1cyclo, 12:0, 14:0, 16:1, and 14:1 *N*-acyl units (Table S7), which are particularly enriched in the endolipidome (Figure S38). Isomeric Gp-NAEs (**7**) and LPEs (**4**) were distinguished based on their composition of *N*- or *O*-acyl building blocks (Figure S38), MS/MS fragmentation patterns (Figure S39), and the distribution of ^{13}C isotopomers upon mixed isotope labeling by feeding with a 1:1 mixture of [U−^{12}C] and [U−^{13}C]-*E. coli* (Figures S40 and S41). ESI-(+)-HR-MS^E analysis of bacterial food-derived [U−C_n]-LPEs (**4**) with homologous long-chain *O*-acyl side chains, such as 14:0, 16:0, 18:0, 16:1, 18:1, 17:1cyclo, and 19:1cyclo, furnished signals for uniformly [U−^{12}C] and [U−^{13}C] labeled isotopomers (Figure S40 and Table S5), in agreement with their origin from partial hydrolysis of bacterial phosphatidylethanolamines (**6**, PE). In contrast, ESI-(+)-HR-MS^E of the Gp-NAEs (**7**) such as Gp-NAE-15:1cyclo (**17**) (Figure 6a) furnished signals corresponding to [U−^{12}C], [$^{13}C_5$], [$^{13}C_{15}$], and [U−$^{13}C_{20}$] isotopomers for the molecular ion $[C_{20}H_{41}NO_7P]^+$, as well as signals for [U−^{12}C], [$^{13}C_2$], [$^{13}C_{15}$], and [U−$^{13}C_{17}$] isotopomers of the [C_{15},C_2]-labeled *N*-acyl ethanolamine fragment ion $[C_{17}H_{32}NO]^+$ (Figure 6b and Figure S41). These results demonstrate that [C_{15},C_5]-Gp-NAE-15:1cyclo (**17**) is biosynthesized by the nematode through attachment of the (chain-shortened) bacteria-derived [C_{15}]-15:1cyclo *N*-acyl unit to an uniformly labeled [C_5]-glycerylphosphoethanolamine building block (presumably via *N*-acylation of PEs (**3**) to furnish NAPEs (**5**)), which places the biosynthesis of Gp-NAEs (**7**) upstream of NAEs (**1**) as well as SNAPs (**8**) and GNAPs (**9**). While these results demonstrate the integration of (chain-shortened) bacteria-derived *N*-acyl units into endometabolome enriched Gp-NAEs (**7**), homologous series with medium-length *N*-acyl units ranging from 8 to 14 carbons have previously been described in starved *C. elegans* L1 larvae utilizing ethanol as sole carbon source,[61] indicating that in the absence of bacterial lipids, the Gp-NAEs (**7**) can also be produced by de novo lipogenesis. Their *daf-22* dependence has previously been described,[33] but their potential function as intermediates in *C. elegans*' NAE biosynthesis has not yet been demonstrated.

Targeted ESI-(+)-HR-MS/MS screening for the corresponding *lyso*-NAPEs (**6**) in the *C. elegans* lipidome revealed the presence of multiple homologous series (Figures 6c and S42) that could be distinguished from the isomeric phosphatidylethanolamines (PEs, **3**) based on their MS/MS fragmentation patterns (Figure S43) and composition of (*N*- or) *O*-acyl units. *Lyso*-NAPEs carrying 15:1cyclo as the *N*-acyl unit (**18**) (Figure 6a) and branched-chain iso-fatty acids such as 15:0iso and 17:0iso as *O*-acyl unit are particularly abundant in the *C. elegans* lipidome (Figure S42), demonstrating that *lyso*-NAPE-dependent *N*-acyl ethanolamine metabolism also includes chain-shortened fatty acid building blocks.

Characterization of 2-(β-Glucosyl)-glyceryl *N*-Acyl Phosphoethanolamines (GGp-NAEs)

Having identified Gp-NAEs (**7**) like Gp-NAE-15:1cyclo (**17**) (Figure 6a) as potential intermediates in NAE (**1**), SNAP (**8**), and GNAP (**9**) biosynthesis, we screened for additional modular metabolites carrying these building blocks. ESI-(+)-HR-MS/MS analysis of the exometabolome extract highlighted a series of structurally related modular 2-(β-glucosyl)-glyceryl *N*-acyl phosphoethanolamines (GGp-NAEs, **10**) carrying homologous *N*-acyl moieties ranging from 10 to 20 carbons (see Table S8 for 39 assigned structures), some of which have previously been detected.[23,33,61] Comparative LC-MS analysis indicated that these GGp-NAEs (**10**) are abundant in hermaphroditic *C. elegans*, *C. briggsae*, *C. tropicalis*, as well as gonochoristic *C. brenneri*, *C. remanei*, and *C. wallacei*. In contrast to male-produced SNAP (**8**), the biosynthesis of GGp-NAEs (**10**) in gonochoristic *Caenorhabditis* species is not sex-specific (Figure S44). The highly unsaturated GGp-NAE 20:5 ($\Delta^{5,8,11,14,17}$) (**20**) (Figure 6a), an amphiphilic derivative of the endocannabinoid *N*-eicosapentaenoyl ethanolamine (NAE 20:5), constitutes the most abundant GGp-NAE (**10**) representative in *C. elegans* (Figure 6f) and related nematodes. Dominating GGp-NAEs were enriched from 4 L of a *C. elegans* liquid culture medium and the structures of GGp-NAE-15:1cyclo ($\Delta^{7,8}$) (**19**), GGp-NAE-20:5 ($\Delta^{5,8,11,14,17}$) (**20**), and GGp-NAE-18:5 ($\Delta^{3,6,9,12,15}$) (**21**) were established by one and two-dimensional NMR spectroscopy (Figure 6a and Table S2). Comparative analysis of exo- and endometabolome extracts demonstrated that release rates of the strongly retained Gp-NAEs (**7**) are dramatically increased upon conversion to the corresponding 2-*O*-β-glucosides (GGp-NAEs, **10**) (Figure 6d), suggesting that 2-*O*-glucosylation converts them into amphiphilic environmental signals. In contrast to GGp-NAE-20:5

https://doi.org/10.1021/acsbiomedchemau.5c00012
ACS Bio Med Chem Au 2025, 5, 602−619

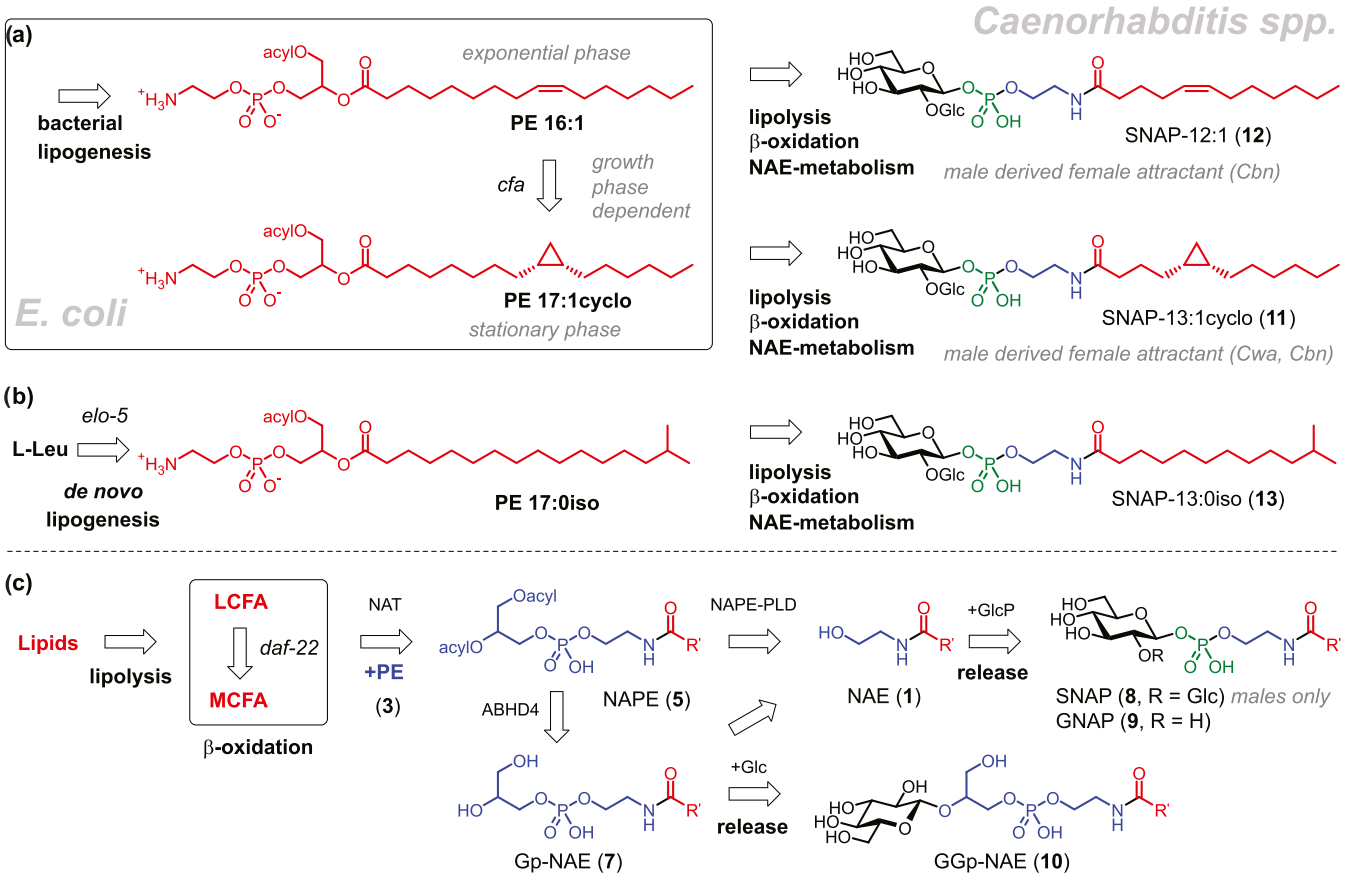

Figure 7. (a) Biogenesis of *β*-glycosyl *N*-acyl phosphoethanolamines in *Caenorhabditis* spp. involves the integration of fatty acid building blocks from growth phase-dependent bacterial lipogenesis, as well as (b) *elo-5*-dependent de novo lipogenesis, along with lipolysis, peroxisomal *β*-oxidation via *daf-22* and NAE metabolism; (c) biosynthetic pathway from exogenous or endogenous lipids to *β*-glycosyl *N*-acyl phosphoethanolamines involves lipolysis and chain shortening of resulting long-chain fatty acids (LCFAs) by *daf-22*-dependent peroxisomal-*β*-oxidation to furnish medium-chain fatty acids (MCFAs), which are attached to phosphatidylethanolamines (PE, **3**) by *N*-acyltransferases (*NAT*) to furnish *N*-acyl phosphatidylethanolamines (NAPEs, **5**). Hydrolysis of NAPEs provides *N*-acyl *lyso*-phosphatidylethanolamines (*lyso*-NAPEs, **6**), glycerylphosphate *N*-acyl ethanolamines (Gp-NAEs, 7), and *N*-acyl ethanolamines (NAEs, **1**), which serve as precursors for the *β*-sophorosyl *N*-acyl ethanolamine phosphates (SNAP, **8**), *β*-glucosyl *N*-acyl ethanolamine phosphates (GNAP, **9**), and 2-*β*-glucosyl glycerylphosphate *N*-acyl ethanolamines (GGp-NAEs, **10**) that are subsequently released into the environment.

(**20**) and GGp-NAE-17:1cyclo, the relative amounts of GGp-NAE-18:5 (**21**) and GGp-NAE-15:1cyclo (**19**) are strongly reduced in the *daf-22(ok693)* mutant metabolome (Figure 6e), which demonstrates that the biosynthesis of these modular metabolites integrates *N*-acyl building blocks derived from the peroxisomal *β*-oxidation of long-chain fatty acid precursors such as 20:5 or *E. coli*-derived 17:1cyclo, respectively. Comparative analysis of GNAP (**9**) and GGp-NAE (**10**) profiles in the *C. elegans* exometabolome indicated that relative abundancies of their *N*-acyl building blocks are similar but not identical (Figure 6f). The eicosapentaenoyl (20:5) unit constitutes the dominating *N*-acyl group for both **9** and **10**, suggesting a potential function in endocannabinoid signaling. Cyclopropyl fatty acids represent another group of dominating *N*-acyl residues, but their distribution differs between GNAPs (**9**) and GGp-NAEs (**10**), with short chains (11:1cyclo, 13:1cyclo, and 15:1cyclo) dominating for GNAPs (**9**), and longer chains (15:1cyclo and 17:1cyclo) dominating for GGp-NAEs (**10**). The same predominance for shorter *N*-acyl moieties for GNAPs (**9**) versus GGp-NAEs (**10**) is also observed for saturated straight and branched-chain components (Figure 6f), indicating that GNAPs (**9**) and GGp-NAEs (**10**) are derived from similar but not identical *N*-aycl ethanolamine pools or that their biosynthesis is carefully controlled.

Biosynthesis of Glycosylated *N*-Acyl Phosphoethanolamines in *Caenorhabditis spp.*

In conclusion, using a combination of comparative metabolomics and stable isotope labeling experiments, the biosynthesis of *β*-glycosylated *N*-acyl phosphoethanolamines (**8**, **9**, **10**) in *Caenorhabditis* spp. was elucidated (Figure 7). Biosynthesis of the two dominating *β*-sophorosyl *N*-acyl phosphoethanolamines SNAP-13:1cyclo (**11**) and SNAP-12:1 (**12**) depends on bacterial lipogenesis and thereby encodes the growth phase of the bacterial food source (Figure 7a). Male-specific biosynthesis of female attracting SNAP-13:1cyclo (**11**) requires bacteria-derived cyclopropyl fatty acids (17:1cyclo or 19:1cyclo), which are exclusively produced upon stationary phase-dependent expression of *E. coli* cyclopropyl fatty acid synthase (*cfa*) that converts all monounsaturated 16:1 and 18:1 into 17:1cyclo and 19:1cyclo, respectively. Because biosynthesis of SNAP-12:1 (**12**) requires the bacteria-derived monounsaturated fatty acids 16:1 and 18:1, sex-specific SNAP-13:1cyclo (**11**) and SNAP-12:1 (**12**) signaling in gonochoristic *Caenorhabditis spp.* encodes information about the availability and growth phase of the bacterial food

https://doi.org/10.1021/acsbiomedchemau.5c00012
ACS Bio Med Chem Au 2025, 5, 602−619

source(s) (Figure 7a). In contrast, the biosynthesis of iso-branched SNAPs such as SNAP-13:0iso (**13**) involves de novo lipogenesis of iso-fatty acids including chain elongation of a L-leucine-derived [C_5]-isovalerate building block via elongase *elo-5*, to furnish long-chain iso-fatty acid precursors (15:0iso and 17:0iso) (Figure 7b).

The various long-chain fatty acid (LCFA) building blocks originating from bacterial lipogenesis or de novo lipogenesis are released by lipolysis (Figure 7c) and potentially enter the *daf-22*-dependent peroxisomal β-oxidation cycle. Resulting medium-chain fatty acids (MCFA) and their LCFA precursors are subsequently utilized for *N*-acylation of phosphatidylethanolamines (PEs, **3**) in a tightly controlled manner to furnish *N*-acyl phosphatidylethanolamines (NAPEs, **5**). NAPEs (**5**) with long and medium-chain *N*-acyl moieties are hydrolyzed, either directly or via the corresponding *lyso*-NAPE (**6**) and Gp-NAE (**7**) intermediates, to furnish lipophilic NAEs (**1**) that act as endogenous signaling molecules,[22] and in addition, also serve as precursors for amphiphilic β-glycosyl *N*-acyl phosphoethanolamines such as the exclusively male-produced SNAPs (**8**), as well as GNAPs (**9**). Furthermore, 2-*O*-β-glucosylation of endometabolome enriched Gp-NAEs (**7**) furnishes the amphiphilic 2-(β-glucosyl)-glyceryl *N*-acyl phosphoethanolamines (GGp-NAEs, **10**) (predominantly 20:5 and 15:1cyclo in *C. elegans*), which are subsequently released into the environment to function as precursors for the corresponding NAEs (**1**), thereby enabling intra- and potentially even interspecies signaling.

DISCUSSION

N-Acyl ethanolamines such as the endocannabinoids NAE-20:5 and NAE-20:4 are known as endogenous lipid signaling molecules that regulate various aspects of *C. elegans* biology, including reproductive development, TGF-β signaling, cholesterol transport, axon regeneration, behavior, and nociception.[22] Our chemical analysis revealed that the structural diversity of homologous *N*-acyl ethanolamines with 55 assigned structures in *C. elegans* and related nematodes is considerably larger than previously anticipated. This structural diversity originates from the integration of diverse fatty acid building blocks derived directly from bacterial lipogenesis, from chain elongation and desaturation of bacteria-derived precursors (mainly palmitic acid, 16:0), or from *elo-5*-dependent de novo lipogenesis of iso-fatty acids by the nematode. Structural diversity is further increased by chain shortening of long-chain fatty acids via the *daf-22*-dependent peroxisomal β-oxidation cycle, demonstrating that NAE signaling involves building blocks from anabolic and catabolic pathways. Because biological activities of endocannabinoid signals depend most strongly on the homologous *N*-acyl side chains, the structural diversity of NAE metabolites might be paralleled by a yet undisclosed functional diversity.

Furthermore, our results demonstrate that the lipophilic *N*-acyl ethanolamines serve as building blocks for three classes of amphiphilic nematode-derived modular metabolites (NDMMs), including 17 members of β-sophorosyl *N*-acyl phosphoethanolamines (SNAPs, **8**), 46 members of β-glucosyl *N*-acyl phosphoethanolamines (GNAPs, **9**) and 39 members of 2-(β-glucosyl)-glyceryl *N*-acyl phosphoethanolamines (GGp-NAEs, **10**). While these compounds are conserved in *Caenorhabditis*, their individual compound profiles are highly species-specific.

Comparative analysis of exo- and endometabolomes revealed that the lipophilic NAE (**1**) and Gp-NAE (**7**) precursors are retained in the endolipidome, whereas conversion into the amphiphilic *O*-glycosyl derivates, SNAPs (**8**), GNAPs (**9**), and GGp-NAEs (**10**) results in their subsequent release into the exometabolome, thus suggesting potential signaling functions. Behavioral assays revealed that ecologically relevant amounts of the predominantly male-produced SNAP-13:1cyclo (**11**) retains females of gonochoristic *C. wallacei*. Females of *C. brenneri* are retained by both SNAP-13:1cyclo (**11**) and SNAP-12:1 (**12**), indicating species-specific communication. In addition, it is conceivable that the various glycosylated *N*-acyl phosphoethanolamines, SNAP (**8**), GNAP (**9**), and GGp-NAEs (**10**), elicit additional biological activities on nematode development or behavior that have not yet been characterized. Considering their accumulation in the exometabolome, facile hydrolysis, and the fact that water-soluble *N*-acyl phosphoethanolamines (**2**) have previously been described as prodrugs for *N*-acyl ethanolamine (**1**) based endocannabinoids,[62] the glycosylated *N*-acyl phosphoethanolamines (**8**, **9**, **10**) might represent a general mechanism for endogenous *N*-acyl ethanolamine signaling to be shared with the environment, and thus potentially be involved in the regulation of intra and interspecies interactions. Additional bioassays to characterize the potential bioactivities of the amphiphilic glycosylated *N*-acyl phosphoethanolamines (**8**, **9**, and **10**) and their role as precursors for lipophilic *N*-acyl ethanolamines will be required to evaluate their ecological significance.

The female retention by male-produced SNAP-13:1cyclo (**11**) in *C. wallacei* depends on the presence of the cyclopropyl moiety derived exclusively from the bacterial food source, which provides further evidence for the importance of bacterial cyclopropyl fatty acids in the chemical signaling of bacterivorous nematodes. We have previously shown that female production of the highly species-specific male attracting sex-pheromone fasc-C4-cycloC11 (SMID: fasc#1) in *C. remanei* depends on bacteria-derived 17:1cyclo and 19:1cyclo produced by *E. coli* upon entering the stationary growth phase.[63] Its biosynthetic intermediate, 11:1cyclo (SMID: becyp#1) has subsequently been identified as an endogenous activator of *fat-7* expression in *C. elegans*.[64] In contrast, the monounsaturated palmitoleic acid (18:1 (Δ^9)), which serves as a precursor for 19:1cyclo in *E. coli* and is dominating its lipidome during the exponential growth phase, enhances recovery of *C. elegans* dauer larva.[65] Growth phase-dependent cyclopropanation of unsaturated fatty acids is prominent among bacteria[66,67] and abundant within the *C. elegans* microbiome, as shown by FAME analysis of the "CeMBio" model microbiome,[45] in which 10 out of 12 bacterial isolates were found to be rich in cyclopropyl fatty acids (Figure S29). Retention of *C. wallacei* females by male-produced SNAP-13:1cyclo (**11**), the production of which requires bacterial food-derived 17:1cyclo or 19:1cyclo, thus encodes not only bacterial food availability but also bacterial growth phase-dependent fatty acid cyclopropanation as a widespread indicator for the exhaustive conversion of environmental nutrients into bacterial biomass, which is required to make these resources accessible for bacterivorous nematodes. Taken together, our results demonstrate how the metabolism, development, and behavior of bacterivorous nematodes like the *Caenorhabditis* spp. are shaped by the lipid composition of its bacterial food source.

https://doi.org/10.1021/acsbiomedchemau.5c00012
ACS Bio Med Chem Au 2025, 5, 602−619

Characterization of dietary and lipogenesis pathways along with complementary chain shortening via peroxisomal β-oxidation in *N*-acyl ethanolamine biosynthesis represents an important step toward understanding the metabolic regulation of the lipid and endocannabinoid network. Additional species-specific glycosylation of endogenous NAEs and their subsequent release into the environment facilitates intraspecies and potentially even interspecies interactions via amphiphilic exocannabinoid signaling molecules.

EXPERIMENTAL PROCEDURES

Organisms

All *Caenorhabditis* nematode strains, including the wild-type isolates of *C. elegans* N2 (United Kingdom), *C. wallacei* JU1904 (Indonesia), *C. brenneri* PB2801 (Costa Rica), *C. briggsae* AF16 (India), *C. nigoni* JU1422 (India), *C. remanei* PB4641 (United States), and *C. tropicalis* JU1373 (La Réunion), as well as the *C. elegans* knockout mutants *daf-22(ok693)*strain RB859, *kat-1(tm1037)* strain VS24, *elo-5(gk208)* strain VC410, and *him-5(e1490)* strain DR466, were obtained from the Caenorhabditis Genetics Center (CGC). The uracil auxotroph *E. coli* strain OP50 and the CeMBio[45] bacterial strains *Enterobacter hormaechei* (CEent1), *Lelliottia amnigena* (JUb66), *Acinetobacter guillouiae* (MYb10), *Sphingomonas molluscorum* (JUb134), *Stenotrophomonas indicatrix* (JUb19), *Pseudomonas lurida* (MYb11), *Pseudomonas berkeleyensis* (MSPm1), *Comamonas piscis* (BIGb0172), *Pantoea nemavictus* (BIGb0393), *Ochrobactrum vermis* (MYb71), *Sphingobacterium multivorum* (BIGb0170), and *Chryseobacterium scophthalmum* (JUb44) were obtained from the Caenorhabditis Genetics Center (CGC). The Δ*leu* Δ*ile* Δ*val* auxotroph *B. subtilis ilvB2 leuA169* strain GB7044 was obtained from the Bacillus Genetics Strain Center (BGSC 1A452). The Δ*leu* Δ*ile* Δ*val* auxotroph *E. coli* BL21(DE3) Δ*ilvD* Δ*leuB* Δ*avtA* Δ*ilvE* was generated by Yojiro Ishida (Rutgers University).

Cultivation of *E. coli* and *B. subtilis*

E. coli OP50 and *B. subtilis* GB7044 were precultured on solidified Lysogeny Broth agar (15.0 g/L agar with 10.0 g/L tryptone, 5.0 g/L yeast extract, 5.0 g/L NaCl) at 37 °C for 12 h, and single colonies were used to inoculate 1.0 L of Lysogeny Broth medium, which was incubated overnight (12−14 h) at 37 °C and 180 rpm. Bacterial cells were harvested by centrifugation at 4700g for 10 min, washed with M9 phosphate buffer (11.3 g/L $Na_2HPO_4{\cdot}7H_2O$, 5.0 g/L NaCl, 3.0 g/L KH_2PO_4, 247 mg/L $MgSO_4{\cdot}7H_2O$), and stored at 7 °C until being used as food for nematode cultures (maximum of 2 weeks).

Cultivation of CeMBio Bacteria

Bacteria isolated from the *C. elegans* microbiome (CeMBio)[45] were precultured on solidified Lysogeny Broth agar at 25 °C for 12 h, and single colonies were used to inoculate 1.0 L of Lysogeny Broth (LB) medium, which was incubated for 24 h at 25 °C and 180 rpm. Bacterial cells were harvested by centrifugation at 4700*g* for 10 min, washed with M9 phosphate buffer (11.3 g/L $Na_2HPO_4{\cdot}7H_2O$, 5.0 g/L NaCl, 3.0 g/L KH_2PO_4, 247 mg/L $MgSO_4{\cdot}7H_2O$), frozen at −20 °C, and lyophilized for subsequent FAME analysis.

Cultivation of Nematodes

Nematodes were cultivated on solidified Nematode Growth Medium (NGM) agar (15 g/L agar, 2.5 g/L peptone, 3.0 g/L NaCl, 2.71 g/L KH_2PO_4, 0.89 g/L K_2HPO_4, 240 mg/L $MgSO_4{\cdot}7H_2O$, 147 mg/L $CaCl_2{\cdot}2H_2O$, 5 mg cholesterol in 1 mL ethanol, 17.0 g/L agar[68]) seeded with bacterial food. Wild-type isolates of *C. brenneri*, *C. briggsae*, *C. nigoni*, *C. remanei*, *C. tropicalis*, and *C. wallacei* were cultured at 23 °C, and *C. elegans* wild-type strain N2 and mutants *daf-22(ok693)*, *kat-1(tm1037)*, *elo-5(gk208)*, and *him-5(e1490)* were cultured at 20 °C.

Preparation of Nematode Metabolome Extracts

Mixed stage nematodes from four 10 cm NGM agar plates collected in S-medium were used as inoculums for liquid cultures grown in 100 mL S-medium (5.85 g/L NaCl, 1.0 g/L K_2HPO_4, 6.0 g/L KH_2PO_4, 2.94 g/L K_3[citrate]$\cdot H_2O$, 200 mg/L citric acid$\cdot H_2O$, 738 mg/L $MgSO_4$, 441 mg/L $CaCl_2{\cdot}2H_2O$, 18.6 mg/L Na_2H_2EDTA, 6.9 mg/L $FeSO_4{\cdot}7H_2O$, 2.0 mg/L $MnCl_2{\cdot}4H_2O$, 2.9 mg/L $ZnSO_4{\cdot}7H_2O$, 0.25 mg/L $CuSO_4{\cdot}5H_2O$, 5 mg/L cholesterol[68]) at 150 rpm and 20 °C (for *C. elegans* wild-type and mutant strains) or 23 °C (for all other *Caenorhabditis* species). A 1 cm^3 portion of concentrated *E. coli* OP50 bacterial pellets (from an overnight culture in LB medium at 37 °C) was provided daily as food from day 1 to 7, after which the cultures were starved for an additional 7 days. Nematodes were separated by centrifugation at 1000*g* for 10 min, frozen at −20 °C, lyophilized, powdered by crushing with solid NaCl, and extracted with 3 × 5 mL methanol to furnish the endometabolome extract. The filtered supernatant was frozen at −20 °C, lyophilized, and extracted with 3 × 50 mL methanol for 12 h each to furnish the exometabolome extract. The extracts were filtered, concentrated to dryness under reduced pressure at 40 °C, and reconstituted in 1 mL of methanol. Aliquots were diluted with methanol and analyzed by UHPLC-ESI-HR-MS^E. All measurements were performed by using at least three biological replicates.

Enrichment of Target Compounds

Target compounds were enriched by reverse phase solid phase extraction on 0.5 g of RP-C18 (Chromabond, Macherey-Nagel) using a stepwise gradient of methanol in water as eluent (10 mL each, from 0% to 100% methanol using 10 increments of +10%). The resulting RP-C18 SPE fractions were concentrated under reduced pressure using a Vacufuge Plus Concentrator (Eppendorf), and aliquots were analyzed by UHPLC-ESI-HR-MS.

Isolation of β-Glycosyl *N*-Acyl Phosphoethanolamines (SNAP (8) and GNAP (9))

The β-glycosyl *N*-acyl phosphoethanolamine was enriched from 2 L of the liquid culture supernatant of *C. wallacei* strain JU1904 grown as described before. The filtered supernatant was frozen at −20 °C and lyophilized, and the residue was extracted with 3 × 200 mL of methanol for 12 h each. The combined extract was filtered and concentrated to dryness under reduced pressure at 40 °C. The resulting residue was reconstituted in 10 mL of methanol and filtered to remove insoluble salt. The concentrated exometabolome extract was reconstituted in 5 mL of water and fractionated by reverse phase chromatography on 5 g of RP-C18 cartridges (Chromabond, Macherey-Nagel) using a stepwise gradient of methanol in water as eluent (from 0 to 100% methanol using increments of +10% and fractions of 10 mL). The resulting RP-C18 fractions were concentrated under reduced pressure using a Vacufuge Plus Concentrator (Eppendorf), and aliquots were analyzed by UHPLC-ESI-(−)-HR-MS^E and ^1H NMR. SPE fractions enriched in target compounds (eluted with 70 and 80% methanol) were submitted to semipreparative HPLC using a 1525 EF pump (Waters) connected to a 2487 DAD UV detector (Waters) with a detection wavelength of 305 nm and a FC203B fraction collector (Gilson). Chromatographic separation was achieved using an Xterra MS C18 column (150 mm, 19 mm inner diameter, 5 μm particle size) (Waters). Optimized HPLC conditions were developed on UHPLC and then transferred to semipreparative scale. A water/acetonitrile solvent system was used with 0.05% formic acid at a flow rate of 8 mL/min. The temperature of the column was maintained at 45 °C. Fractions (8 mL) were collected every minute. Aliquots of 10 μL were diluted and analyzed by UHPLC-ESI-(−)-HR-MS^E with isocratic elution. HPLC fractions were concentrated under reduced pressure using a Centrivap vacuum concentrator (Labconco). Fractions rich in target compounds SNAP-13:1cyclo (**11**), SNAP-12:1 (**12**), SNAP-13:0iso (**13**), SNAP-11:0iso (**14**), and GNAP-13:1cyclo (**15**) were dissolved in CD_3OD and analyzed by NMR spectroscopy (Table S1).

Isolation of 2-(β-Glucosyl)-glyceryl *N*-Acyl Phosphoethanolamines (GGp-NAEs, 10)

The 2-(β-glucosyl)-glyceryl *N*-acyl phosphoethanolamines were enriched from 4 L of the liquid culture supernatant of *C. elegans* strain N2 grown as described before. The filtered supernatant was

https://doi.org/10.1021/acsbiomedchemau.5c00012
ACS Bio Med Chem Au 2025, 5, 602−619

frozen at −20 °C and lyophilized, and the residue was extracted with 3 × 200 mL methanol for 12 h each. The combined extract was filtered and concentrated to dryness under reduced pressure at 40 °C. The resulting residue was reconstituted in 10 mL methanol and filtered to remove insoluble salt. The concentrated exometabolome extract was reconstituted in 5 mL water and fractionated by reverse phase chromatography on 5 g RP-C18 cartridges (Chromabond, Macherey-Nagel) using a stepwise gradient of methanol in water as eluent (from 0% to 100% methanol using increments of +10% and fractions of 10 mL). The resulting RP-C18 fractions were concentrated under reduced pressure using a Vacufuge Plus Concentrator (Eppendorf), and aliquots were analyzed by UHPLC-ESI-(−)-HR-MS^E and ^{1}H NMR. SPE fractions enriched in target compounds (eluted with 80% methanol) were submitted to semipreparative HPLC using an LC-20AR pump (Shimadzu, Japan) connected to an SPD-20A UV−vis detector (Shimadzu) with detection at 305 nm and a FRC-40 fraction collector (Shimadzu). Chromatographic separation was achieved using an Xterra MS C18 column (150 mm, 19 mm i.d., 5 μm particle size) (Waters). Optimized HPLC conditions were developed on UHPLC and then transferred to semipreparative scale. A water/acetonitrile solvent system was used with 0.05% formic acid at a flow rate of 8 mL/min. The temperature of the column was maintained at 45 °C. Fractions (8 mL) were collected every minute. Aliquots of 10 μL were diluted and analyzed by UHPLC-ESI-(−)-HR-MS^E with isocratic elution. HPLC fractions were concentrated under reduced pressure using a Centrivap vacuum concentrator (Labconco). Fractions rich in target compounds GGp-NAE-15:1cyclo (**19**), GGp-NAE-20:5 (**20**), and GGp-NAE-18:5 (**21**) were dissolved in CD_3OD and analyzed by NMR spectroscopy (Table S2).

Chemical Correlation by Palladium-Catalyzed Hydrogenation

Aliquots (10 μL) of semipreparative HPLC fractions enriched in *β*-glycosyl *N*-acyl phosphoethanolamines (from separation of the *C. wallacei* JU1904 exometabolome) were diluted with 1 mL ethanol and treated with 10 mg palladium on carbon (10%, w/w), and hydrogen gas was bubbled through the vigorously stirred mixture. After 1 h, the mixtures were filtered over cotton and concentrated under reduced pressure, and the residues were taken up in 100 μL of methanol for comparative UHPLC-ESI-(−)-HR-MS^E analysis using the diluted untreated exometabolome fraction (10 μL in 100 μL of methanol) as control.

Sex-Specific Metabolome Analysis

For sex-specific exometabolome analysis of *C. wallacei* JU1904, *C. brenneri* PB2801, *C. nigoni* JU1422, or *C. remanei* PB4641, a total number of 100 male and 100 female adult nematodes were collected from nonstarved cultures on NGM agar seeded with *E. coli* OP50 using a 0.25 mm platinum−iridium (90:10 wt %) wire pick. Nematodes were incubated for 15 h at 20 °C and 180 rpm in 500 μL of S-medium supplemented with 100 μL of an *E. coli* OP50 overnight culture in LB medium. Cultures were filtered over cotton to remove the nematodes, and the medium was frozen at −20 °C, lyophilized, and extracted with 500 μL methanol. Filtered extracts were concentrated under reduced pressure, and the residues were taken up in 100 μL of methanol for UHPLC-ESI-(−)-HR-MS^E analysis.

Comparative Analysis of Well-Fed and Starved Cultures

Mixed stage nematodes of *C. wallacei* JU1904 or *C. brenneri* PB2801 from four 10 cm agar plates collected in S-medium were used as inoculums for liquid cultures grown in 100 mL of S-medium at 180 rpm and 23 °C. Each day, 1 cm^3 of concentrated *E. coli* OP50 bacterial pellets (from an overnight culture in LB medium at 37 °C) was provided as food from day 1 to 7, after which worms were separated by centrifugation at 1000*g* for 10 min, and the filtered supernatant representing the exometabolome under well-fed conditions was frozen at −20 °C. The separated nematodes were transferred into 100 mL fresh S-medium and cultured for an additional 7 days without food, after which worms were separated again by centrifugation at 1000*g* for 10 min. The filtered supernatant representing the exometabolome under starved conditions was frozen at −20 °C. The remaining nematodes were transferred into 100 mL of fresh S-medium and cultured at 23 °C and 180 rpm for another 7 days without food, after which worms were separated by centrifugation at 1000*g* for 10 min. The filtered supernatant representing the exometabolome under severely starved conditions was frozen at −20 °C. The frozen exometabolome samples were lyophilized and extracted with 3 × 50 mL methanol for 12 h each. The combined extracts were filtered, concentrated to dryness under reduced pressure at 40 °C, and reconstituted in 1 mL of methanol for UHPLC-ESI-(−)-HR-MS^E analysis. All experiments were performed in triplicate.

Comparative Analysis of Exo- and Endometabolomes

Mixed stage *C. wallacei* JU1904 or *C. brenneri* PB2801 from four 10 cm agar plates collected in S-medium were used as inoculums for liquid cultures grown in 100 mL of S-medium at 180 rpm and 23 °C. Each day, 1 cm^3 of concentrated *E. coli* OP50 bacterial pellets (from an overnight culture in LB medium at 37 °C) was provided as food from day 1 to 5, after which worms were separated by centrifugation at 1000*g* for 10 min. The separated nematodes were transferred to 100 mL of fresh S-medium supplemented with 1 cm^3 concentrated *E. coli* OP50 bacterial pellets and cultivated at 23 °C and 180 rpm for 5 h, after which the worm pellet representing the endometabolome was separated by centrifugation (10 min at 4700*g*), frozen at −20 °C, lyophilized, and extracted with 3 × 50 mL of methanol for 12 h each. The filtered supernatant representing the exometabolome was frozen at −20 °C, lyophilized, and extracted with 3 × 50 mL methanol for 12 h each. The combined extract was filtered, concentrated to dryness under reduced pressure at 40 °C, and reconstituted in 1 mL methanol. An aliquot of 50 μL was diluted with 50 μL methanol and submitted for LC-MS analysis. All experiments were performed in triplicate.

Comparative Analysis of Wild-Type and Mutant Metabolomes

C. elegans mutants *daf-22(ok693)* strain RB859, *kat-1(tm1037)* strain VS24, *elo-5(gk208)* strain VC410, and *him-5(e1490)* strain DR466 along with the wild-type strain N2 as control were precultured on NGM agar plates seeded with *E. coli* OP50. Mixed stage nematodes from four 10 cm agar plates collected in S-medium were used as inoculums for liquid cultures grown in 100 mL of S-medium at 150 rpm and 20 °C. 1 cm^3 of *E. coli* OP50 bacterial pellets (from overnight cultures in LB medium) was provided as food from day 1 to 7, and the cultures were starved for an additional 7 days, after which the cultures were harvested and processed as previously described. The harvested nematodes were lyophilized, and their weight was measured for normalization. All measurements were performed in triplicate.

Comparative analysis of *E. coli* and *B. subtilis* Fed Cultures

C. wallacei JU1904 or *C. brenneri* PB2801 were precultured on NGM agar plates seeded with *E. coli* OP50 or *B. subtilis* GB7044. Mixed stage nematodes from four 10 cm agar plates collected in S-medium were used as inoculums for liquid cultures grown in 100 mL of S-medium at 150 rpm and 23 °C. 1 cm^3 of *E. coli* OP50 or *B. subtilis* GB7044 bacterial pellets (from overnight cultures in LB medium) was provided as food from day 1 to 7, and the cultures were starved for an additional 7 days, after which the cultures were harvested and processed as previously described. All measurements were performed in triplicate.

Cultivation of [U−^{12}C]/[U−^{13}C]-*E. coli*

E. coli BL21(DE3) was precultured on solidified M9 minimal salt agar (15.0 g agar/L with 5.0 g/L NaCl, 6.0 g/L Na_2HPO_4, 3.0 g/L KH_2PO_4, 1.0 g/L NH_4Cl, 247 mg/L $MgSO_4{\cdot}7H_2O$, 11.1 mg $CaCl_2{\cdot}2H_2O$, 3.3 mg/L $FeSO_4{\cdot}7H_2O$) supplemented with 5.0 g/L D-glucose at 37 °C for 12 h, and single colonies were used to inoculate 1 L of M9 minimal salt medium supplemented with 5.0 g/L D-glucose. Cultures were incubated overnight (12−14 h) at 37 °C with 180 rpm. Bacterial cells were harvested by centrifugation at 4700*g* for 10 min, washed with M9 phosphate buffer (11.3 g/L $Na_2HPO_4{\cdot}7H_2O$, 5.0 g/L NaCl, 3.0 g/L KH_2PO_4, 247 mg/L $MgSO_4{\cdot}7H_2O$), and

https://doi.org/10.1021/acsbiomedchemau.5c00012
ACS Bio Med Chem Au 2025, 5, 602−619

stored at 7 °C until being used as food for nematode cultures (maximum of 2 weeks). Isotope labeled [U−^{13}C]-*E. coli* was prepared by using D-[U−$^{13}C_6$]-glucose as the sole carbon source.

Mixed [^{12}C]/[^{13}C]-Isotope Labeling Experiments

C. wallacei JU1904 was precultured at 23 °C on solidified peptone-free Nematode Growth Medium (NGM) agar (15 g/L agar, 3.0 g/L NaCl, 2.71 g/L KH_2PO_4, 0.89 g/L K_2HPO_4, 246 mg/L $MgSO_4 \cdot 7H_2O$, 147 mg/L $CaCl_2 \cdot 2H_2O$, 5 mg cholesterol in 1 mL ethanol, 17.0 g/L agar) seeded with a 1:1 mixture (w/w) of natural abundance [U−^{12}C]- and [U−^{13}C]-*E. coli*. Mixed stage nematodes from four 10 cm peptone-free NGM agar plates collected in citrate-free S-medium were used as inoculums for liquid cultures grown in 100 mL of citrate-free S-medium (5.85 g/L NaCl, 1.0 g/L K_2HPO_4, 6.0 g/L KH_2PO_4, 738 mg/L $MgSO_4$, 441 mg/L $CaCl_2 \cdot 2H_2O$, 18.6 mg/L Na_2H_2EDTA, 6.9 mg/L $FeSO_4 \cdot 7H_2O$, 2.0 mg/L $MnCl_2 \cdot 4H_2O$, 2.9 mg/L $ZnSO_4 \cdot 7H_2O$, 0.25 mg/L $CuSO_4 \cdot 5H_2O$, 5 mg/L cholesterol) at 150 rpm and 23 °C. 1 cm^3 portion of a 1:1 mixture (w/w) of natural abundance [U−^{12}C] and [U−^{13}C]-*E. coli* bacterial pellets were provided as food from day 1 to 7. Nematodes were separated by centrifugation at 1000*g* for 10 min, frozen at −20 °C, lyophilized, powdered by crushing with solid NaCl, and extracted with 3 × 5 mL methanol to furnish the endometabolome extract. The filtered supernatant was frozen at −20 °C, lyophilized, and extracted with 3 × 50 mL methanol for 12 h each to furnish the exometabolome extract. The extracts were filtered, concentrated to dryness under reduced pressure at 40 °C, and reconstituted in 1 mL of methanol. Aliquots were diluted with methanol and analyzed by UHPLC-ESI-HR-MS^E. All measurements were performed in triplicate.

Cultivation of L-[U−$^{13}C_5$]-Valine or L-[U−$^{13}C_6$]-Leucine Labeled *E. coli*

E. coli BL21(DE3) Δ*ilvD* Δ*leuB* Δ*avtA* Δ*ilvE* was precultured on solidified (15.0 g/L agar) supplemented M9 minimal salt agar at 37 °C for 12 h and used to inoculate 1 L of M9 minimal salt medium (12.8 g/L g $Na_2HPO_4 \cdot 7H_2O$, 3.0 g/L g KH_2PO_4, 1.0 g/L NH_4Cl, 0.5 g/L NaCl, 240 mg/L $MgSO_4 \cdot 7H_2O$, 14.7 mg $CaCl_2 \cdot 2H_2O$) supplemented with 5.0 g/L D-glucose as carbon source, as well as L-valine (20 mg/L), L-leucine (20 mg/L), L-isoleucine (20 mg/L), and kanamycin (50 mg/L). Cultures were incubated overnight (12−14 h) at 37 °C with 180 rpm. Bacterial cells were harvested by centrifugation at 4700*g* for 10 min, washed with M9 phosphate buffer (11.3 g/L $Na_2HPO_4 \cdot 7H_2O$, 5.0 g/L NaCl, 3.0 g/L KH_2PO_4, 247 mg/L $MgSO_4 \cdot 7H_2O$), and stored at 7 °C until being used as food for nematode cultures. L-[U−$^{13}C_5$]-Valine and L-[U−$^{13}C_6$]-leucine labeled *E. coli* was prepared by substituting the corresponding amino acid supplement with a 1:1 mixture (w/w) of natural abundance [U−^{12}C] and the [U−^{13}C]-labeled isotopomer.

Incorporation of L-[U−$^{13}C_5$]-Valine and L-[U−$^{13}C_6$]-Leucine Labeled *E. coli*

C. brenneri PB2801 was precultured on peptone-free NGM agar seeded with natural abundance *E. coli* BL21(DE3) Δ*ilvD* Δ*leuB* Δ*avtA* Δ*ilvE* as control or a 1:1 mixture (w/w) of natural abundance and L-[U−$^{13}C_5$]-valine or L-[U−$^{13}C_6$]-leucine labeled *E. coli* BL21-(DE3) Δ*ilvD* Δ*leuB* Δ*avtA* Δ*ilvE*. Mixed stage nematodes from four 10 cm agar plates collected in S-medium were used as inoculums for liquid cultures grown in 100 mL S-medium at 150 rpm and 23 °C. 1 cm^3 of natural abundance or a 1:1 mixture (w/w) of natural abundance and L-[U−$^{13}C_5$]-valine or L-[U−$^{13}C_6$]-leucine labeled *E. coli* BL21(DE3) Δ*ilvD* Δ*leuB* Δ*avtA* Δ*ilvE* bacterial pellets was provided as food from day 1 to 7, after which the cultures were harvested and processed as previously described. All measurements were performed in triplicate.

Incorporation of [H]- & [D_6]-17:0iso by *C. elegans elo-5(gk208)*

C. elegans elo-5(gk208) strain VC410 was repeatedly axenized using egg bleaching[68] to remove the concomitant *Stenotrophomonas* bacterium that supports its growth. Eggs were hatched on NGM agar seeded with *E. coli* OP50 and supplemented with 10 mM 17:0iso (1 mL of 2.7 mg/mL of fatty acid in EtOH per 9 mL of *E. coli* OP50 culture) synthesized as previously described.[49] Monoxenic conditions were established by L1 developmental arrest of the F2 generation after being depleted of the 17:0iso supplement. L1 arrested nematodes were subsequently rescued by transfer to plates with 10 mM 17:0iso or [D_6]-17:0iso. Nematodes were precultured for 4 rounds on NGM agar seeded with *E. coli* OP50 supplemented with 10 mM 17:0iso or [D_6]-17:0iso. Mixed stage nematodes from six 6 cm agar plates collected in S-medium were used as inoculums for liquid cultures grown in 100 mL of S-medium at 180 rpm and 23 °C. Each day, 0.5 cm^{3}of concentrated *E. coli* OP50 bacterial pellets (from an overnight culture in LB medium at 37 °C) supplemented with 1 mM 17iso or [D_6]-17iso was provided as food from day 1 to 5, after which the cultures were harvested and processed as previously described. All experiments were performed in triplicate.

Lipid Extraction of Nematodes

Lyophilized nematodes (10 mg dry weight) were treated with 1.7 mL methyl *tert*-butyl methyl ether (MTBE), and samples were vortexed vigorously.[69] Worms were sonicated for 30 min at 0 °C, treated with 0.42 mL of water, and sonicated for another 15 min. Phases were separated by centrifugation at 4 °C and 4700*g* for 15 min. The upper organic phase was transferred to a 4 mL glass vial, and the remaining lower phase was re-extracted with an additional 1.7 mL of MTBE for 15 min. After centrifugation, the organic layers were combined and evaporated under reduced pressure. The residue was dissolved in 0.1 mL ACN/iPrOH/water (65:30:5, v/v/v) at a final concentration of 100 mg dry worms/mL and analyzed by UHPLC-ESI-HR-MS. All measurements were performed in triplicate.

Preparation of Fatty Acid Methyl Esters (FAMEs)

Lyophilized nematodes or bacteria (10 mg dry weight) were treated with 1 mL of 2.5% (v/v) sulfuric acid in methanol and incubated at 70 °C for 2 h. After cooling to room temperature, 1.5 mL water and 0.2 mLhexane were added. The mixture was vortexed for 30 s and centrifuged at 1000*g* for 5 min. The upper organic layer was separated and utilized for fatty acid methyl ester analysis by GC-EIMS.

Gas Chromatography Electron Ionization Mass Spectrometry (GC-EIMS)

Gas chromatography electron ionization mass spectrometry (GC-EIMS) was performed using a GC 7890B (Agilent) coupled with a Gerstel Multi-Purpose Sampler (MPS) and connected to an MSD 5977A mass spectrometer (Agilent). Chromatographic separations were achieved using an HP 5 ms Ultra Inert column (30 m, 0.25 mm ID, 0.25 μm film thickness) with helium as the carrier gas at a flow rate of 1 mL/min. A temperature program starting at 50 °C for 5 min, followed by a linear gradient of +10 °C/min to 320 and 320 °C for 10 min, was used. A total volume of 1 μL was injected spitless at an injector temperature of 270 °C. 70 eV mass spectra were acquired from m/z 35−650 amu. Instruments were controlled by using Gerstel Maestro software (V1). Data were processed using MassHunter software version B.07 (2014) from Agilent Technologies.

Liquid Chromatography Mass Spectrometry (LC-MS)

Ultrahigh-performance liquid chromatography electrospray ionization high-resolution tandem mass spectrometry (UHPLC-ESI-HR-MS/MS) analyses were performed using an Acquity ultrahigh-pressure liquid chromatography (UHPLC) system coupled to a Synapt G2 QTOF mass spectrometer (Waters, Milford, MA) controlled by MassLynx 4.1 software. Chromatographic separations were achieved using a Waters Acquity HSS T3 UHPLC column (100 mm × 2.1 mm, 1.8 μm particle diameter) with a flow rate of 500 μL/min using a binary solvent mixture composed of eluent A (water containing 0.05% formic acid) and eluent B (98% acetonitrile and 2% water containing 0.05% formic acid). A linear gradient from 0 to 100% B in 10 min was applied, followed by a hold at 100% for 5 min and re-equilibration at 0% B for another 5 min. Analysis was performed using electrospray ionization (ESI) in positive and negative ionization modes using a source temperature of 120 °C, desolvation gas at 15 L/min and 450 °C, and capillary voltage at 2.5 kV for ESI-(+) or 2.0 kV for ESI-(−).

https://doi.org/10.1021/acsbiomedchemau.5c00012
ACS Bio Med Chem Au 2025, 5, 602−619

Mass spectra were recorded from m/z 50 to m/z 1200. Fragmentation data were collected in data-independent (broad band collision induced dissociation) mode using a collision energy of 8-55 V in positive mode and 10−60 V in negative mode. Data were analyzed with MassLynx software (Waters, Milford, MA).

Nuclear Magnetic Resonance Spectroscopy (NMR)

NMR spectra were recorded at 400 MHz for ^{1}H and 100 MHz for ^{13}C using a Bruker AVANCE II 400 instrument equipped with a 5 mm BBFO+ probe or at 600 MHz for ^{1}H and 125 MHz for ^{13}C using a Bruker Ascend 600 instrument with a 5 mm BBI probe (NPAC, UniNE). CD_3OD (99.96% or 99.8% D) or $CDCl_3$ (99.8% D) was used as the solvent. Residual solvent signals were used as an internal reference with ^{1}H at 3.31 ppm and ^{13}C at 49.05 ppm for CD_3OD or ^{1}H at 7.26 ppm and ^{13}C at 77.16 ppm for $CDCl_3$. Two-dimensional high-resolution double quantum filtered (*dqf*)-COSY spectra were recorded using the *cosydfph* pulse sequence with phase cycling for coherence selection by acquiring 32 scans (NS 64 for GNAP) using 8192 data points along f2 and 256 increments along f1 for a sweep width of 7.5 ppm. HSQC spectra were recorded using the *hsqcetgpsi2* pulse sequence by acquiring 448 scans using 1024 data points in f2 and 64 increments in f1. HMBC spectra were recorded by using the *hmbcgpndqf* pulse sequence by acquiring 432 scans using 2048 data points in f2 and 128 increments in f1. Spectra were zero-filled to 8192 × 512 for COSY, 2048 × 128 for HSCQ, and 2048 × 128 for HMBC prior to Fourier transformation and then phased manually and baseline corrected if required. Post processing and data analysis were performed using the TopSpin 4.1.3 (2021, Bruker Biospin), MestReNova 9.0.0 (2013, Mestrelab Research), and MestReNova 14.1.2 (2020, Mestrelab Research) software.

Retention Assay

Nematode preference for environments conditioned with known amounts of SNAP-13:1cyclo (**11**) or SNAP-12:1 (**12**) was measured by using a retention assay with *C. wallacei* JU1904 and *C. brenneri* PB2801. On a 6 cm Petri dish filled with 6 mL peptone-free NGM agar, circular scoring regions with 9 mm diameter were marked. Next, 1 μL of 10% aqueous methanol (as solvent control) or solutions of SNAP-13:1cyclo (**11**) and of SNAP-12:1 (**12**) in biologically relevant concentrations ranging from 10 nM−10 μM in 10% aqueous methanol were placed in the center of the scoring areas and left to dry for 5 min. Young adult nematodes from nonstarved and noncrowded 6 cm NGM agar plates seeded with *E. coli* OP50 were separated by sex and transferred to peptone-free NGM agar without food for approximately 1 h before being used for the experiment in order to minimize the amount of concomitant bacteria. Individual worms were placed into the center of the conditioned scoring region, and the time required for the nematodes to leave the scoring region was recorded. Nematodes were defined to have left the scoring area when no part of their body was within the circular boundary. A total number of 20 worms per condition were analyzed, and experiments were repeated at least twice on separate days. A Welch's t test was performed using SPSS Statistics software version 26 (IBM) to evaluate the effect of β-glycosyl N-acyl phosphoethanolamines on mean times nematode spent in scoring regions.

■ ASSOCIATED CONTENT

Supporting Information

The Supporting Information is available free of charge at https://pubs.acs.org/doi/10.1021/acsbiomedchemau.5c00012.

Phylogeny of *Caenorhabditis* species; HR-MS/MS spectra of SNAPs and GNAPS; hydrolysis of SNAPs ; chemical correlations via micro reactions; sex-specific analysis; bacterial food-dependent analysis; release rates; comprative analysis of endo- and exo-emetabolomes; MS spectra for isotopomers from stable isotope labelling experiments; MS fragmentation pathways; NAE and lyso-NAPE profiling; NMR and MS data; retention assay data; and NMR spectra (PDF)

■ AUTHOR INFORMATION

Corresponding Author

Stephan H. von Reuß − *Laboratory for Bioanalytical Chemistry, University of Neuchâtel, CH-2000 Neuchâtel, Switzerland; Neuchatel Platform for Analytical Chemistry (NPAC), University of Neuchâtel, CH-2000 Neuchâtel, Switzerland;* orcid.org/0000-0003-4325-5495; Email: stephan.vonreuss@unine.ch

Authors

Siva Bandi − *Laboratory for Bioanalytical Chemistry, University of Neuchâtel, CH-2000 Neuchâtel, Switzerland;* orcid.org/0000-0001-9653-4610

Marie-Désirée Schlemper-Scheidt − *Laboratory for Bioanalytical Chemistry, University of Neuchâtel, CH-2000 Neuchâtel, Switzerland;* orcid.org/0000-0002-4616-7784

Rocío Rivera Sánchez − *Laboratory for Bioanalytical Chemistry, University of Neuchâtel, CH-2000 Neuchâtel, Switzerland;* orcid.org/0000-0002-0502-2159

Sylvain Sutour − *Neuchatel Platform for Analytical Chemistry (NPAC), University of Neuchâtel, CH-2000 Neuchâtel, Switzerland;* orcid.org/0000-0001-9676-7123

Gaétan Glauser − *Neuchatel Platform for Analytical Chemistry (NPAC), University of Neuchâtel, CH-2000 Neuchâtel, Switzerland;* orcid.org/0000-0002-0983-8614

Yojiro Ishida − *Center for Advanced Biotechnology and Medicine (CABM), Rutgers University, Piscataway, New Jersey 08854, United States*

Complete contact information is available at: https://pubs.acs.org/10.1021/acsbiomedchemau.5c00012

Author Contributions

[‖]S.B. and M.D.S.S. contributed equally to this work. S.B., M.D.S.S., R.R.S., and S.v.R conceived the study, designed experiments, and analyzed the data. S.B., R.R.S., M.D.S.S., S.S., and G.G. performed experiments. R.R.S. and Y.I. provided research materials. S.v.R., S.B., and M.D.S. wrote the manuscript with contributions from all authors. All authors have given approval to the final version of the manuscript.

Funding

Financial support by the Swiss National Science Foundation (SNSF-169700; SNSF-197228) and the University of Neuchâtel (UniNE) is gratefully acknowledged.

Notes

The authors declare no competing financial interest.

■ ACKNOWLEDGMENTS

The authors thank Dr. Armelle Vallat (Neuchâtel Platform for Analytical Chemistry, NPAC) for GC-EIMS measurements. *C. elegans* mutants *daf-22(ok693)*, *kat-1(tm1037)*, *elo-5(gk208)*, and *him-5(e1490)* were generated by the International *C. elegans* Gene Knockout Consortium, which is gratefully acknowledged. All nematode strains were provided by the Caenorhabditis Genetics Center, which is funded by the NIH Office of Research Infrastructure Programs (P40 OD010440).

REFERENCES

(1) Elphick, M. R.; Egertová, M.The Phylogenetic Distribution and Evolutionary Origins of Endocannabinoid Signalling. In *Handbook of Experimental Pharmacology*; Springer, 2005; Vol. *168*, pp 283−297.

(2) Blancaflor, E. B.; Kilaru, A.; Keereetaweep, J.; Khan, B. R.; Faure, L.; Chapman, K. D. *N*-Acyl ethanolamines: lipid metabolites with functions in plant growth and development. *Plant J.* **2014**, *79* (4), 568−583.

(3) Silver, R. J. The Endocannabinoid System of Animals. *Animals* **2019**, *9*, 686.

(4) Cannon, A. E.; Chapman, K. D. Lipid Signaling through G Proteins. *Trends Plant Sci.* **2021**, *26* (7), 720−728.

(5) Syed, S. K.; Bui, H. H.; Beavers, L. S.; Farb, T. B.; Ficorilli, J.; Chesterfield, A. K.; Kuo, M. S.; Bokvist, K.; Barrett, D. G.; Efanov, A. M. Regulation of GPR119 receptor activity with endocannabinoid-like lipids. *Am. J. Physiol.-Endocrinol. Metab.* **2012**, *303* (12), E1469−E1478.

(6) Im, D. S. GPR119 and GPR55 as Receptors for Fatty Acid Ethanolamides, Oleoylethanolamide and Palmitoylethanolamide. *Int. J. Mol. Sci.* **2021**, *22* (3), 1034.

(7) Movahed, P.; Jönsson, B. A.; Birnir, B.; Wingstrand, J. A.; Jørgensen, T. D.; Ermund, A.; Sterner, O.; Zygmunt, P. M.; Högestätt, E. D. Endogenous unsaturated C18 *N*-acyl ethanolamines are vanilloid receptor (TRPV1) agonists. *J. Biol. Chem.* **2005**, *280* (46), 38496−38504.

(8) Thabuis, C.; Tissot-Favre, D.; Bezelgues, J. B.; Martin, J. C.; Cruz-Hernandez, C.; Dionisi, F.; Destaillats, F. Biological functions and metabolism of oleoylethanolamide. *Lipids* **2008**, *43* (10), 887−894.

(9) Hansen, H. S.; Diep, T. A. *N*-acyl ethanolamines, anandamide and food intake. *Biochem. Pharmacol.* **2009**, *78* (6), 553−560.

(10) Leung, D.; Saghatelian, A.; Simon, G. M.; Cravatt, B. F. Inactivation of *N*-acyl phosphatidylethanolamine phospholipase D reveals multiple mechanisms for the biosynthesis of endocannabinoids. *Biochemistry* **2006**, *45* (15), 4720−4726.

(11) Liu, J.; Wang, L.; Harvey-White, J.; Osei-Hyiaman, D.; Razdan, R.; Gong, Q.; Chan, A. C.; Zhou, Z.; Huang, B. X.; Kim, H. Y.; Kunos, G. A biosynthetic pathway for anandamide. *Proc. Natl. Acad. Sci. U.S.A.* **2006**, *103* (36), 13345−13350.

(12) Ueda, N.; Tsuboi, K.; Uyama, T. Metabolism of endocannabinoids and related *N*-acyl ethanolamines: canonical and alternative pathways. *FEBS J.* **2013**, *280* (9), 1874−1894.

(13) Rahman, I. A. S.; Tsuboi, K.; Uyama, T.; Ueda, N. New players in the fatty acyl ethanolamide metabolism. *Pharmacol. Res.* **2014**, *86*, 1−10.

(14) Tsuboi, K.; Okamoto, Y.; Rahman, I. A.; Uyama, T.; Inoue, T.; Tokumura, A.; Ueda, N. Glycerophosphodiesterase GDE4 as a novel lysophospholipase D: a possible involvement in bioactive N-acyl ethanolamine biosynthesis. *Biochim. Biophys. Acta, Mol. Cell Biol. Lipids* **2015**, *1851* (5), 537−548.

(15) Lee, H. C.; Simon, G. M.; Cravatt, B. F. ABHD4 regulates multiple classes of N-acyl phospholipids in the mammalian central nervous system. *Biochemistry* **2015**, *54* (15), 2539−2549.

(16) Ogura, Y.; Parsons, W. H.; Kamat, S. S.; Cravatt, B. F. A calcium-dependent acyltransferase that produces *N*-acyl phosphatidylethanolamines. *Nat. Chem. Biol.* **2016**, *12* (9), 669−671.

(17) Tsuboi, K.; Takezaki, N.; Ueda, N. The *N*-acyl ethanolamine-hydrolyzing acid amidase (NAAA). *Chem. Biodivers.* **2007**, *4* (8), 1914−1925.

(18) Ueda, N.; Tsuboi, K.; Uyama, T. *N*-acyl ethanolamine metabolism with special reference to *N*-acyl ethanolamine-hydrolyzing acid amidase (NAAA). *Prog. Lipid Res.* **2010**, *49* (4), 299−315.

(19) Yue, Y.; Li, S.; Shen, P.; Park, Y. *Caenorhabditis elegans* as a model for obesity research. *Curr. Res. Food Sci.* **2021**, *4*, 692−697.

(20) An, L.; Fu, X.; Chen, J.; Ma, J. Application of *Caenorhabditis elegans* in Lipid Metabolism Research. *Int. J. Mol. Sci.* **2023**, *24* (2), 1173.

(21) Vrablik, T. L.; Watts, J. L. Polyunsaturated fatty acid derived signaling in reproduction and development: insights from *Caenorhabditis elegans* and *Drosophila melanogaster*. *Mol. Reprod. Dev.* **2013**, *80* (4), 244−259.

(22) Estrada-Valencia, R.; de Lima, M. E.; Colonnello, A.; Rangel-López, E.; Saraiva, N. R.; de Ávila, D. S.; Aschner, M.; Santamaría, A.The Endocannabinoid System in *Caenorhabditis elegans*. In *Reviews of Physiology, Biochemistry and Pharmacology*; Springer, 2023; Vol. *184*, pp 1−31.

(23) Helf, M. J.; Fox, B. W.; Artyukhin, A. B.; Zhang, Y. K.; Schroeder, F. C. Comparative metabolomics with Metaboseek reveals functions of a conserved fat metabolism pathway in *C. elegans*. *Nat. Commun.* **2022**, *13* (1), 782.

(24) Abdollahi, M.; Castaño, J. D.; Salem, J. B.; Beaudry, F. Anandamide Modulates Thermal Avoidance in *Caenorhabditis elegans* Through Vanilloid and Cannabinoid Receptor Interplay. *Neurochem. Res.* **2024**, *49* (9), 2423−2439.

(25) Levichev, A.; Faumont, S.; Berner, R. Z.; Purcell, Z.; White, A. M.; Chicas-Cruz, K.; Lockery, S. R. The conserved endocannabinoid anandamide modulates olfactory sensitivity to induce hedonic feeding in *C. elegans*. *Curr. Biol.* **2023**, *33* (9), 1625−1639.e4.

(26) Galles, C.; Prez, G. M.; Penkov, S.; Boland, S.; Porta, E. O. J.; Altabe, S. G.; Labadie, G. R.; Schmidt, U.; Knölker, H. J.; Kurzchalia, T. V.; de Mendoza, D. Endocannabinoids in *Caenorhabditis elegans* are essential for the mobilization of cholesterol from internal reserves. *Sci. Rep.* **2018**, *8* (1), 6398.

(27) Lehtonen, M.; Reisner, K.; Auriola, S.; Wong, G.; Callaway, J. C. Mass-spectrometric identification of anandamide and 2-arachidonoylglycerol in nematodes. *Chem. Biodivers.* **2008**, *5* (11), 2431−2441.

(28) Lucanic, M.; Held, J. M.; Vantipalli, M. C.; Klang, I. M.; Graham, J. B.; Gibson, B. W.; Lithgow, G. J.; Gill, M. S. *N*-acyl ethanolamine signalling mediates the effect of diet on lifespan in *Caenorhabditis elegans*. *Nature* **2011**, *473* (7346), 226−229.

(29) Annibal, A.; Karalay, Ö.; Latza, C.; Antebi, A. A novel EI-GC/MS method for the accurate quantification of anti-aging compound oleoylethanolamine in *C. elegans*. *Anal. Methods* **2018**, *10* (22), 2551−2559.

(30) Harrison, N.; Lone, M. A.; Kaul, T. K.; Rodrigues, P. R.; Ogungbe, I. V.; Gill, M. S. Characterization of *N*-acyl phosphatidylethanolamine-specific phospholipase-D isoforms in the nematode *Caenorhabditis elegans*. *PLoS One* **2014**, *9* (11), e113007.

(31) Pastuhov, S. I.; Matsumoto, K.; Hisamoto, N. Endocannabinoid signaling regulates regenerative axon navigation in *Caenorhabditis elegans* via the GPCRs NPR-19 and NPR-32. *Genes Cells* **2016**, *21* (7), 696−705.

(32) Izrayelit, Y.; Robinette, S. L.; Bose, N.; von Reuss, S. H.; Schroeder, F. C. 2D NMR-based metabolomics uncovers interactions between conserved biochemical pathways in the model organism *Caenorhabditis elegans*. *ACS Chem. Biol.* **2013**, *8* (2), 314−319.

(33) Artyukhin, A. B.; Zhang, Y. K.; Akagi, A. E.; Panda, O.; Sternberg, P. W.; Schroeder, F. C. Metabolomic "Dark Matter" Dependent on Peroxisomal β-Oxidation in *Caenorhabditis elegans*. *J. Am. Chem. Soc.* **2018**, *140* (8), 2841−2852.

(34) Bouagnon, A. D.; Lin, L.; Srivastava, S.; Liu, C. C.; Panda, O.; Schroeder, F. C.; Srinivasan, S.; Ashrafi, K. Intestinal peroxisomal fatty acid β-oxidation regulates neural serotonin signaling through a feedback mechanism. *PLoS Biol.* **2019**, *17* (12), e3000242.

(35) (a) Félix, M.-A.; Braendle, C.; Cutter, A. D. A streamlined system for species diagnosis in Caenorhabditis (Nematoda: Rhabditidae) with name designations for 15 distinct biological species. *PLoS One* **2014**, *9* (4), No. e94723; Erratum in: (b) *PLoS One* **2015**, *10* (3), e0118327.

(36) Stuart, L. J.; Buck, J. P.; Tremblay, A. E.; Buist, P. H. Configurational analysis of cyclopropyl fatty acids isolated from *Escherichia coli*. *Org. Lett.* **2006**, *8* (1), 79−81.

(37) Hodgkin, J.; Horvitz, H. R.; Brenner, S. Nondisjunction Mutants of the Nematode *Caenorhabditis elegans*. *Genetics.* **1979**, *91* (1), 67−94.

https://doi.org/10.1021/acsbiomedchemau.5c00012
ACS Bio Med Chem Au 2025, 5, 602−619

(38) Choe, A.; von Reuss, S. H.; Kogan, D.; Gasser, R. B.; Platzer, E. G.; Schroeder, F. C.; Sternberg, P. W. Ascaroside signaling is widely conserved among nematodes. *Curr. Biol.* **2012**, *22* (9), 772−780.
(39) Dong, C.; Reilly, D. K.; Bergame, C.; Dolke, F.; Srinivasan, J.; von Reuss, S. H. Comparative Ascaroside Profiling of *Caenorhabditis* Exometabolomes Reveals Species-Specific (ω) and (ω - 2)-Hydroxylation Downstream of Peroxisomal β-Oxidation. *J. Org. Chem.* **2018**, *83* (13), 7109−7120.
(40) Perez, C. L.; Van Gilst, M. R. A 13C isotope labeling strategy reveals the influence of insulin signaling on lipogenesis in *C. elegans*. *Cell Metab.* **2008**, *8* (3), 266−274.
(41) Ratnappan, R.; Amrit, F. R.; Chen, S. W.; Gill, H.; Holden, K.; Ward, J.; Yamamoto, K. R.; Olsen, C. P.; Ghazi, A. Germline signals deploy NHR-49 to modulate fatty-acid β-oxidation and desaturation in somatic tissues of *C. elegans*. *PLoS Genet.* **2014**, *10* (12), e1004829.
(42) Dancy, B. C. R.; Chen, S. W.; Drechsler, R.; Gafken, P. R.; Olsen, C. P. 13C- and 15N-Labeling Strategies Combined with Mass Spectrometry Comprehensively Quantify Phospholipid Dynamics in *C. elegans*. *PLoS One.* **2015**, *10* (11), e0141850.
(43) Hoang, K. L.; Gerardo, N. M.; Morran, L. T. The effects of *Bacillus subtilis* on *Caenorhabditis elegans* fitness after heat stress. *Ecol. Evol.* **2019**, *9* (6), 3491−3499.
(44) Nickels, J. D.; Chatterjee, S.; Mostofian, B.; Stanley, C. B.; Ohl, M.; Zolnierczuk, P.; Schulz, R.; Myles, D. A. A.; Standaert, R. F.; Elkins, J. G.; Cheng, X.; Katsaras, J. *Bacillus subtilis* Lipid Extract, A Branched-Chain Fatty Acid Model Membrane. *J. Phys. Chem. Lett.* **2017**, *8* (17), 4214−4217.
(45) Dirksen, P.; Assié, A.; Zimmermann, J.; Zhang, F.; Tietje, A. M.; Marsh, S. A.; Félix, M. A.; Shapira, M.; Kaleta, C.; Schulenburg, H.; Samuel, B. S. CeMbio - The *Caenorhabditis elegans* Microbiome Resource. *G3:Genes, Genomes, Genet.* **2020**, *10* (9), 3025−3039.
(46) Zhu, H.; Shen, H.; Sewell, A. K.; Kniazeva, M.; Han, M. A novel sphingolipid-TORC1 pathway critically promotes postembryonic development in *Caenorhabditis elegans*. *Elife* **2013**, *2*, e00429.
(47) Zhu, H.; Sewell, A. K.; Han, M. Intestinal apical polarity mediates regulation of TORC1 by glucosylceramide in *C. elegans*. *Genes Dev.* **2015**, *29* (12), 1218−1223.
(48) Kniazeva, M.; Zhu, H.; Sewell, A. K.; Han, M. A Lipid-TORC1 Pathway Promotes Neuronal Development and Foraging Behavior under Both Fed and Fasted Conditions in *C. elegans*. *Dev. Cell* **2015**, *33* (3), 260−271.
(49) Sánchez, R. R.; Bandi, S.; Scheidt, M.-D.; Laaroussi, H.; Fox, B. W.; Ishida, Y.; Glauser, G.; Sutour, S.; von Reuss, S. H. iso-Fatty Acid Metabolism in *Caenorhabditis elegans'* Ceramide Biosynthesis. *Helv. Chim. Acta* **2023**, *106* (11), e202300131.
(50) Hannich, J. T.; Mellal, D.; Feng, S.; Zumbuehl, A.; Riezman, H. Structure and conserved function of iso-branched sphingoid bases from the nematode *Caenorhabditis elegans*. *Chem. Sci.* **2017**, *8* (5), 3676−3686.
(51) Tanno, H.; Sassa, T.; Sawai, M.; Kihara, A. Production of branched-chain very-long-chain fatty acids by fatty acid elongases and their tissue distribution in mammals. *Biochim. Biophys. Acta, Mol. Cell Biol. Lipids* **2021**, *1866* (1), 158842.
(52) Kniazeva, M.; Crawford, Q. T.; Seiber, M.; Wang, C. Y.; Han, M. Monomethyl branched-chain fatty acids play an essential role in *Caenorhabditis elegans* development. *PLoS Biol.* **2004**, *2*, E257.
(53) Kniazeva, M.; Euler, T.; Han, M. A branched-chain fatty acid is involved in post-embryonic growth control in parallel to the insulin receptor pathway and its biosynthesis is feedback-regulated in *C. elegans*. *Genes Dev.* **2008**, *22* (15), 2102−2110.
(54) Richardson, M. B.; Williams, S. J. A practical synthesis of long-chain iso-fatty acids (iso-C12-C19) and related natural products. *Beilstein J. Org. Chem.* **2013**, *9*, 1807−1812.
(55) Golden, J. W.; Riddle, D. L. A gene affecting production of the *Caenorhabditis elegans* dauer-inducing pheromone. *Mol. Gen. Genet.* **1985**, *198* (3), 534−536.
(56) Butcher, R. A.; Ragains, J. R.; Li, W.; Ruvkun, G.; Clardy, J.; Mak, H. Y. Biosynthesis of the *Caenorhabditis elegans* dauer pheromone. *Proc. Natl. Acad. Sci. U.S.A.* **2009**, *106* (6), 1875−1879.
(57) Joo, H. J.; Yim, Y. H.; Jeong, P. Y.; Jin, Y. X.; Lee, J. E.; Kim, H.; Jeong, S. K.; Chitwood, D. J.; Paik, Y. K. *Caenorhabditis elegans* utilizes dauer pheromone biosynthesis to dispose of toxic peroxisomal fatty acids for cellular homoeostasis. *Biochem. J.* **2009**, *422* (1), 61−71.
(58) Mak, H. Y.; Nelson, L. S.; Basson, M.; Johnson, C. D.; Ruvkun, G. Polygenic control of *Caenorhabditis elegans* fat storage. *Nat. Genet.* **2006**, *38* (3), 363−368.
(59) von Reuss, S. H.; Bose, N.; Srinivasan, J.; Yim, J. J.; Judkins, J. C.; Sternberg, P. W.; Schroeder, F. C. Comparative Metabolomics Reveals Biogenesis of Ascarosides, a Modular Library of Small-Molecule Signals in *C. elegans*. *J. Am. Chem. Soc.* **2012**, *134* (3), 1817−1824.
(60) von Reuss, S. H.; Dolke, F.; Dong, C. Ascaroside Profiling of *Caenorhabditis elegans* Using Gas Chromatography-Electron Ionization Mass Spectrometry. *Anal. Chem.* **2017**, *89* (19), 10570−10577.
(61) Artyukhin, A. B.; Yim, J. J.; Cheong Cheong, M.; Avery, L. Starvation-induced collective behavior in *C. elegans*. *Sci. Rep.* **2015**, *5*, 10647.
(62) Juntunen, J.; Huuskonen, J.; Laine, K.; Niemi, R.; Taipale, H.; Nevalainen, T.; Pate, D. W.; Järvinen, T. Anandamide prodrugs. 1. Water-soluble phosphate esters of arachidonylethanolamide and R-methanandamide. *Eur. J. Pharm. Sci.* **2003**, *19* (1), 37−43.
(63) Dolke, F.; Dong, C.; Bandi, S.; Paetz, C.; Glauser, G.; von Reuß, S. H. Ascaroside Signaling in the Bacterivorous Nematode *Caenorhabditis remanei* Encodes the Growth Phase of Its Bacterial Food Source. *Org. Lett.* **2019**, *21* (15), 5832−5837.
(64) Fox, B. W.; Helf, M. J.; Burkhardt, R. N.; Artyukhin, A. B.; Curtis, B. J.; Palomino, D. F.; Schroeder, A. F.; Chaturbedi, A.; Tauffenberger, A.; Wrobel, C. J. J.; Zhang, Y. K.; Lee, S. S.; Schroeder, F. C. Evolutionarily related host and microbial pathways regulate fat desaturation in *C. elegans*. *Nat. Commun.* **2024**, *15* (1), 1520.
(65) Kaul, T. K.; Reis Rodrigues, P.; Ogungbe, I. V.; Kapahi, P.; Gill, M. S. Bacterial fatty acids enhance recovery from the dauer larva in *Caenorhabditis elegans*. *PLoS One* **2014**, *9* (1), e86979.
(66) Grogan, D. W.; Cronan, J. E., Jr Cyclopropane ring formation in membrane lipids of bacteria. *Microbiol. Mol. Biol. Rev.* **1997**, *61* (4), 429−441.
(67) Cronan, J. E. Bacterial membrane lipids: where do we stand. *Annu. Rev. Microbiol.* **2003**, *57*, 203−224.
(68) Stiernagle, T. Maintenance of *C. elegans*. In *C. elegans Research Community*; WormBook, 2006 http://www.wormbook.org/chapters/www_strainmaintain/strainmaintain.html.
(69) Matyash, V.; Liebisch, G.; Kurzchalia, T. V.; Shevchenko, A.; Schwudke, D. Lipid extraction by methyl-*tert*-butyl ether for high-throughput lipidomics. *J. Lipid Res.* **2008**, *49* (5), 1137−1146.

https://doi.org/10.1021/acsbiomedchemau.5c00012
ACS Bio Med Chem Au 2025, 5, 602−619